Identification of Compounds Containing Novel Hydride Ions by Nuclear Magnetic Resonance Spectroscopy

Randell L. Mills
Bala Dhandapani
Mark Nansteel
Jiliang He
Andreas Voigt

BlackLight Power, Inc.
493 Old Trenton Road
Cranbury, NJ 08512

Novel inorganic alkali and alkaline earth hydrides of the formula MH^*, MH_2^*, and MH^*X wherein M is the metal, X, is a halide, and H^* comprises a novel high binding energy hydride ion were synthesized in a high temperature gas cell by reaction of atomic hydrogen with a catalyst and MH, MH_2, or MX corresponding to an alkali metal or alkaline earth metal compound, respectively. Novel hydride ions of the corresponding novel hydride compounds were characterized by an extraordinary upfield shifted peak observed by ^1H nuclear magnetic resonance spectroscopy.

INTRODUCTION

Based on the solution of a Schrödinger-type wave equation with a nonradiative boundary condition based on Maxwell's equations, Mills [1-31] predicts that atomic hydrogen may undergo a catalytic reaction with certain atomized elements or certain gaseous ions which singly or multiply ionize at integer multiples of the potential energy of atomic hydrogen, $27.2\,eV$. For example, potassium atoms ionize at an integer multiple of the potential energy of atomic hydrogen, $m \cdot 27.2\,eV$. The enthalpy of ionization of K to K^{3+} has a net enthalpy of reaction of $81.7426\,eV$, which is equivalent to $m=3$ [32]. The reaction involves a nonradiative energy transfer to form a hydrogen atom that is lower in energy than unreacted atomic hydrogen. The product hydrogen atom has an energy state that corresponds to a fractional principal quantum number. Recent analysis of mobility and spectroscopy data of individual electrons in liquid helium show direct experimental confirmation that electrons may have fractional principal quantum energy levels [33]. The lower-energy hydrogen atom is a highly reactive intermediate which further reacts to form a novel hydride ion. Emission was observed previously from a continuum state of Cs^{2+} and Ar^{2+} at $53.3\,nm$ and $45.6\,nm$, respectively [4]. The single emission feature with the absence of the other corresponding Rydberg series of lines from these species confirmed the resonate nonradiative energy transfer of $27.2\,eV$ from atomic hydrogen to atomic cesium or Ar^{+}. The catalysis product, a lower-energy hydrogen atom, was predicted to be a highly reactive intermediate which further reacts to form a novel hydride ion. The predicted hydride ion of hydrogen catalysis by either cesium atom or Ar^{+} catalyst is the hydride ion $H^{-}(1/2)$. This ion was observed spectroscopically at $407\,nm$ corresponding to its predicted binding energy of $3.05\,eV$. The catalytic reaction with the formation the hydride ions are given in the Appendix.

Prior studies support the possibility of a novel reaction of atomic hydrogen which produces an anomalous discharge and produces novel hydride compounds. Experiments that confirm the novel hydrogen chemistry include extreme ultraviolet (EUV) spectroscopy [2-4, 6-7, 9-17], plasma formation [2-17], power generation [2-3, 5, 10, 31], and analysis of chemical compounds [13, 15-31]. For examples: 1.) Lines

observed by EUV spectroscopy could be assigned to transitions of atomic hydrogen to lower energy levels corresponding to lower energy hydrogen atoms and the emission from the excitation of the corresponding hydride ions [7, 11, 13, 15-17]. 2.) The chemical interaction of catalysts with atomic hydrogen at temperatures below 1000 K has shown surprising results in terms of the emission of the Lyman and Balmer lines [2-17] and the formation of novel chemical compounds [13, 15-31]. 3.) An energetic plasma in hydrogen was generated by a catalysis reaction at 1% of the theoretical or prior known voltage requirement and with 1000's of times less power input in a system wherein the plasma reaction was controlled with a weak electric field [2-3, 10]. 4.) The optically measured output power of gas cells for power supplied to the glow discharge increased by over two orders of magnitude depending on the presence of less than 1% partial pressure of certain of catalysts in hydrogen gas or argon-hydrogen gas mixtures [5]. 5.) A hydrogen plasma formed by reacting a catalyst with hydrogen was recorded when there was no electric energy input to the reaction which confirms a new chemical source of power [8-9].

Typically the emission of extreme ultraviolet light from hydrogen gas is achieved via a discharge at high voltage, a high power inductively coupled plasma, or a plasma created and heated to extreme temperatures by RF coupling (e.g. $>10^6\,K$) with confinement provided by a toroidal magnetic field. Observation of intense extreme ultraviolet (EUV) emission has been reported at low temperatures (e.g. $\approx 10^3\,K$) from atomic hydrogen and certain atomized elements or certain gaseous ions [2-17]. The only pure elements that were observed to emit EUV were those wherein the ionization of t electrons from an atom to a continuum energy level is such that the sum of the ionization energies of the t electrons is approximately $m \cdot 27.2\,eV$ where t and m are each an integer. Potassium, cesium, and strontium atoms and Rb^+ ion ionize at integer multiples of the potential energy of atomic hydrogen and caused emission. Whereas, the chemically similar atoms, sodium, magnesium and barium, do not ionize at integer multiples of the potential energy of atomic hydrogen and caused no emission. An anomalous plasma with hydrogen/potassium mixtures has been reported wherein the plasma decayed with a two second half-life which was the thermal decay time of the filament which

dissociated molecular hydrogen to atomic hydrogen when the electric field was set to zero [8-9]. This experiment showed that hydrogen line emission was occurring even though the voltage between the heater wires was set to and measured to be zero and indicated that the emission was due to a reaction of potassium atoms with atomic hydrogen.

Reports of the formation of novel compounds provide substantial evidence supporting a novel reaction of hydrogen as the mechanism of the observed EUV emission and anomalous discharge. Novel hydrogen compounds have been isolated as products of the reaction of atomic hydrogen with atoms and ions identified as catalysts in the reported EUV studies [2-31]. Novel inorganic alkali and alkaline earth hydrides of the formula MH^* and MH^*X wherein M is the metal, X, is a singly negatively charged anion, and H^* comprises a novel high binding energy hydride ion were synthesized in a high temperature gas cell by reaction of atomic hydrogen with a catalyst such as potassium metal and MH, MX or MX_2 corresponding to an alkali metal or alkaline earth metal compound, respectively [18, 21]. Novel hydride compounds were identified by 1.) time of flight secondary ion mass spectroscopy which showed a dominant hydride ion in the negative ion spectrum, 2.) X-ray photoelectron spectroscopy which showed novel hydride peaks and significant shifts of the core levels of the primary elements bound to the novel hydride ions, 3.) ^1H nuclear magnetic resonance spectroscopy (NMR) which showed extraordinary upfield chemical shifts compared to the NMR of the corresponding ordinary hydrides, and 4.) thermal decomposition with analysis by gas chromatography, and mass spectroscopy which identified the compounds as hydrides [18, 21].

An upfield shifted NMR peak is consistent with a hydride ion with a smaller radius as compared with ordinary hydride since a smaller radius increases the shielding or diamagnetism. Thus, the NMR shows that the hydride formed in the catalytic reaction has been reduced in distance to the nucleus indicating that the electrons are in a lower-energy state. Compared to the shift of known corresponding hydrides the NMR provides direct evidence of reduced energy state hydride ions. We report that novel hydride ions of the corresponding novel hydride compounds of the formula MH^*, MH_2^*, and MH^*X were synthesized by a reaction of potassium or rubidium catalyst and atomic hydrogen. The

compounds showed extraordinary upfield shifted NMR peaks. The synthesis and analysis was shown to be reproducible. Several NMR instruments at independent centers were used to demonstrate the reproducibility of the unique upfield NMR peaks which corresponded to and identified novel hydride ions.

EXPERIMENTAL

Synthesis

A series of novel alkali and alkaline earth hydrides and alkali halido hydrides were synthesized by reaction of atomic hydrogen with a catalyst. The series KH^*Cl, KH^*Br, and KH^*I was synthesized from the corresponding alkali halide KCl (Alfa Aesar ACS grade 99+%), KBr (Alfa Aesar 99.9%), KI (Aldrich Chemical Company 99.9 %) using potassium metal (Aldrich Chemical Company 99%) as the catalyst. KH^* was synthesized from KH (Aldrich Chemical Company 99%) using potassium metal as the catalyst. RbH^*F was synthesized from RbF (Alfa Aesar 99.9%) using potassium metal as the catalyst. RbH^*I was synthesized from RbI (Alfa Aesar 99.9%) using rubidium metal (Aldrich Chemical Company 99%) which is a catalyst as a hydride having Rb^+. CaH_2^* was synthesized using CaH_2 (Alfa Aesar 99.9%) and potassium metal as the catalyst. In the analytical analyses, each starting compound was also used as a control.

Each compound was prepared in a stainless steel gas cell shown in Figure 1 comprising a Ni screen hydrogen dissociator (Belleville Wire Cloth Co., Inc.), catalyst, and alkali halide or alkaline earth hydride. The 316-stainless steel cell was in the form of a tube having an internal cavity of 375 millimeters in length and 140 millimeters in diameter. The wall thickness was 6.35 mm. The bottom of the cell was closed by a 6.35 mm thick circular plate of 316 stainless steel that was welded to the cylinder. The top end of the cell was welded to a bored-through 304 stainless steel conflat-type flange with 8 in. nominal diameter. A mating blank flange was bolted to the bored-through flange with 20 silver-plated bolts. A flange gasket was silver-plated copper. A 1.27 cm OD tube was welded into a hole at the center of the blank flange. This tube was closed at one end and extended 20 cm into the reactor, serving as a thermowell. A 9.5 mm OD stainless steel tube was welded to the flange

approximately 4 cm from the flange center. This tube served as the vacuum line from the cell as well as a hydrogen or helium supply line to the cell.

The reactor was heated in a 10 kW refractory brick kiln (L & L Kiln Model JD230). The kiln had three heating zones and a heated floor that were each heated by separate radiant elements. The zone temperatures were independently controlled by a Dynatrol controller. The reactor was instrumented with 5 type-K thermocouples. Two thermocouples were located in the central thermowell at approximately reactor mid-height and at flange-level. Three thermocouples were fixed to the external surface of the reactor and were located near the base, at mid-height, and near flange-level. The reactor was connected through bellows-type valves to a turbo vacuum pump. The vacuum level was measured by a 0 - 100 torr Baratron vacuum gauge. Pressures above 100 torr were measured by standard dial-type pressure gauges. Temperature and pressure data was logged to a data acquisition system at 5 minute intervals.

Approximately 290 g of nickel screen (0.5 mm wire, 2 mm mesh) was placed circumferentially around the reactor inner wall of the cell. In an environmental chamber under argon gas, about 50 mmoles of dry alkali halide or alkaline earth hydride were placed in a stainless steel crucible on the reactor base. 1 mmole of metallic catalyst was placed in a smaller stainless steel crucible and this crucible was placed in the larger one with the alkali halide or alkaline earth hydride. The reactor was sealed and placed in the kiln. The system was evacuated for 2.5 hours. The reactor was pressurized with hydrogen gas to a pressure of 10 torr and sealed. The kiln was heated to 650 °C at the rate of 300 °C/h. The reactor was held at 650 °C for 72 hours. Hydrogen was added to the system periodically to maintain a pressure level of 10 torr. The reactor was then evacuated for 1 hour while at 650 °C. The kiln and reactor were cooled to room temperature by forced convection in about 2 hours while pumping continued. At room temperature the system was filled with helium gas to a pressure of 1.3 bar. The sealed reactor was then opened in the environmental chamber. NMR samples were placed in glass ampules, sealed with a rubber septa, and transferred out of the chamber to be flame sealed in atmosphere.

NMR Spectroscopy

^1H MAS NMR was performed on solid samples of $KH*Cl$, $KH*Br$, $KH*I$, $KH*$, $RbH*F$, $RbH*I$, and CaH_2^* at Spectral Data Services, Inc., Champaign, Illinois. The data was obtained on a custom built spectrometer operating with a Nicolet 1280 computer. Final pulse generation was from a tuned Henry radio amplifier. The ^1H NMR frequency was 270.6196 MHz. A 5 μsec pulse corresponding to a 41° pulse length and a 3 second recycle delay were used. The window was $\pm 20\ kHz$. The spin speed was 4.0 kHz. (The spin speed was varied to confirm real peaks versus side bands. The latter changed position with spin speed, the former were independent of spin speed.) The number of scans was 600. The offset was 1541.6 Hz, and the magnetic flux was 6.357 T.

The samples were handled under a inert atmosphere. Chemical shifts were referenced to external tetramethylsilane (TMS). To eliminate the possibility that the alkali halide MX influenced the local environment of the ordinary alkali hydride MH to produce an NMR resonance that was shifted upfield relative to MH alone, controls comprising MH and an equimolar MH/MX mixture were run. The reference of each novel hydride comprised the corresponding ordinary hydride MH or MH_2 (Aldrich Chemical Company 99%) and equivalent molar mixtures of MH and MX prepared in a glove box under argon. In the case of the references of $RbHF$ and $RbH*I$, RbH was synthesized by reaction of rubidium metal (Aldrich Chemical Company 99%) with 2 atmospheres of hydrogen in the gas cell at 300 °C for 8 hours.

To confirm that the upfield shifted peak of the $KH*Cl$ samples was reproducible when recorded on different instruments, ^1H MAS NMR was performed on solid samples of $KH*Cl$ and $KH*I$ at four additional independent laboratories The data were recorded on a Bruker DSX-400 spectrometer at 400.13 MHz at the National Research Council of Canada, a Bruker DSX-300 spectrometer at 300.132 MHz at the University of Massachusetts, a Bruker MSL-300 spectrometer at 300.13 MHz at the University of Delaware, and Chemagnetics CMX Infinity 400 spectrometer at 359.7539 MHz at Grace Davison.

^1H MAS NMR was performed on *KH*I* (blue crystals) at the National Research Council of Canada. The data were recorded on a Bruker DSX-400 spectrometer at 400.13 MHz. Samples were packed in zirconia rotors and sealed with airtight O-ring caps under an inert atmosphere. The MAS frequency was 4.5 kHz. During data acquisition, the sweep width was 60.06 kHz; the dwell time was 8.325 μsec, and the acquisition time was 0.03415 sec/scan. The number of scans was typically 32 or 64. Chemical shifts were referenced to external tetramethylsilane (TMS). The reference comprised *KH* (Aldrich Chemical Company 99%).

^1H MAS NMR was performed on solid samples of *KH*Cl* at the University of Massachusetts. The data were recorded on a Bruker DSX-300 spectrometer at 300.132 MHz. Samples were packed and sealed in 5 mm diameter NMR tubes under an inert atmosphere. The samples were spun at a MAS frequency of 4.1 kHz. During data acquisition, the 90 degree pulse length for a single pulse ^1H excitation was 3.4 μsec; the sweep width was 147.058 kHz; the dwell time was 5.5 μsec, and the acquisition time was 0.0139764 sec/scan. The number of scans was typically 32.

^1H MAS NMR was performed on solid samples of *KH*Cl* and *KH*I* (green crystals) at the University of Delaware. The data were recorded on a Bruker MSL-300 spectrometer at 300.13 MHz. Samples were packed and sealed in 5 mm diameter NMR tubes under an inert atmosphere. The samples were spun at a MAS frequency of 3 kHz. During data acquisition, the 90 degree pulse length for a single pulse ^1H excitation was 4 μsec; the dwell time was 5 μsec, and the acquisition time was 5120 μsec/*scan*. The number of scans was typically 540.

^1H MAS NMR was performed on solid samples of *KH*Cl* and *KH*I* (blue crystals) at Grace Davison. The data were recorded on a Chemagnetics CMX Infinity 400 spectrometer at 359.7539 MHz. Each sample was packed and sealed in a 4 mm diameter Chemagnetics probe under an inert atmosphere. The samples were spun at a MAS frequency of 12 kHz. During data acquisition, the 90 degree pulse length for a single pulse ^1H excitation was 4.0 μsec; the spectrum window was ±20 *kHz*; the dwell time was 50 μsec, the recovery delay was 15 μsec, and the acquisition time was 2930 μsec/*scan*. The number of scans was typically 1024.

RESULTS AND DISCUSSION

A. NMR of Potassium Chloro Hydride Sample

The ^1H MAS NMR spectra of six $KH*Cl$ samples from independent syntheses, the control comprising an equal molar mixture of KH and KCl, and the control KH relative to external tetramethylsilane (TMS) are shown in Figures 2A-H, respectively. Ordinary hydride ion has a resonance at 1.1 ppm and 0.8 ppm in the KH/KCl mixture and in KH alone as shown in Figures 2G and 2H, respectively. The sharp peak at 4.3 ppm and the broad peak at 6 ppm shown in Figure 2G are assigned to water in the KCl crystal and to $KHCO_3$ formed from air exposure of K during sample handling, respectively. The broad peak at 4.6 ppm shown in Figure 2H is assigned KOH formed from air exposure of KH during sample handling.

The presence of KCl does not shift the resonance of ordinary hydride as shown in Figure 2G. The resonance at 1.1 ppm which is assigned to ordinary hydride ion was observed in the spectrum of each $KH*Cl$ sample as shown in Figures 2A-F. The distinct 0.8 and 1.1 ppm resonances could not be resolved if they were present. A large distinct upfield resonance was observed in each case at -4.4 to -4.6 ppm which was not observed in either control. The upfield peak in each sample is assigned to a novel hydride ion of $KH*Cl$.

B. NMR of Potassium Bromo Hydride Sample

The ^1H MAS NMR spectra of the $KH*Br$ sample, the control comprising an equal molar mixture of KH and KBr, and the control KH relative to external tetramethylsilane (TMS) are shown in Figures 3A-C, respectively. Ordinary hydride ion has a resonance at 1.1 ppm and 0.8 ppm in the KH/KBr mixture and in KH alone as shown in Figures 3B and 3C, respectively. The additional sharp peaks at 4.3 ppm and 5.9 ppm shown in Figure 3A are assigned to water and $KHCO_3$ formed from air exposure of K during sample handling. The additional sharp peak at 4.2

ppm shown in Figure 3B is assigned to water in the *KBr* crystals. The additional broad peak at 4.6 ppm shown in Figure 3C is assigned *KOH* formed from air exposure of *KH* during sample handling.

The presence of *KBr* does not shift the resonance of ordinary hydride. The resonance at 1.2 ppm which is assigned to ordinary hydride ion was observed in the spectrum of the *KH*Br* sample as shown in Figure 3A. The distinct 0.8 and 1.1 ppm resonances could not be resolved if they were present. A large distinct upfield resonance was observed at -4.1 ppm which was not observed in either control. This upfield shifted peak is assigned to a novel hydride ion of *KH*Br*.

C. NMR of Potassium Iodo Hydride Sample

With an increase of the time of synthesis Mills et al. [18] report that a first blue crystalline compound is formed from the reaction of potassium catalyst with *KI*. With an increase in reaction time the product becomes increasingly green colored. NMR resonances at -1.209 ppm and possibly at -2.5 ppm (See Figure 15) are observed in the case of the blue crystals, and the resonance shifts further upfield to -2.5 ppm as the compound becomes more green colored as shown in Figure 4. These NMR results as well as the previously reported [18] liquid chromatography and X-ray photoelectron spectroscopy data support the production of two distinct hydride ions with different binding energies. This may be due to the ability of two potassium ions as well as a potassium atom to catalyze atomic hydrogen to different energy states as shown in the Appendix. In the present study, the NMR was obtained on blue crystal, light green crystals, and dark green crystals which formed with a reaction time of progressively longer duration.

The ^{1}H MAS NMR spectra of *KH*I* samples from separate syntheses of longer duration relative to external tetramethylsilane (TMS) is shown in Figure 4A-C. Distinguishable upfield resonances were observed at -3.2, -2.5, and -1.8 ppm for the dark green crystals, the green crystals, and the blue crystals as shown in Figure 4A-C, respectively. The upfield peak in each sample is assigned to a novel hydride ion of *KH*I*. The down field shifted peaks may be ordinary hydride in a different chemical environment.

The presence of *KI* does not shift the resonance of ordinary hydride. Ordinary hydride ion has a resonance at 1.1 ppm and 0.8 ppm in the *KH/ KI* mixture and in *KH* alone as shown in Figures 4D and 4E, respectively. The additional peaks at 4.5 to 4.6 ppm are assigned to *KOH* formed from air exposure of *KH* during sample handling.

D. Comparison of NMR of Potassium Iodo Hydride and Potassium Chloro Hydride Samples at Independent Laboratories

To confirm that the upfield shifted peaks of the *KH*Cl* and *KH*I* samples were reproducible when recorded on different instruments, ^1H MAS NMR was performed on solid samples of *KH*Cl* and *KH*I* at four additional independent laboratories. The spectra are shown in Figures 9-17 and the results are summarized in Table 1. The ^1H MAS NMR spectra of six *KH*Cl* samples from independent syntheses shown in Figures 2A-F are in agreement with the independently obtained results run on *KH*Cl* samples as given in Table 1. Two different novel hydride ions were reported by Mills et al. [18] in the case of the *KH*I* samples. The ^1H MAS NMR spectra of the *KH*I* blue crystal sample shown in Figure 4C and the light green sample shown in Figure 4B are in agreement with the independently obtained results run on corresponding samples as given in Table 1. These results demonstrate that the upfield shifted peaks are reproducible and that they can not be attributed to instrument artifact.

E. NMR of Potassium Hydride Sample

The ^1H MAS NMR spectra of the *KH** sample and control *KH* relative to external tetramethylsilane (TMS) are shown in Figures 5A and 5B, respectively. Ordinary hydride ion has a resonance at 1.1 ppm and 0.8 ppm in *KH* as shown in Figure 5B. The peak at 4.1 ppm shown in Figure 5A is assigned to water. The additional broad peak at 4.6 ppm shown in Figure 5B is assigned *KOH* formed from air exposure of *KH* during sample handling. The spin speed was varied to confirm real peaks versus side bands. The latter changed position with spin speed, the former were independent of spin speed. The peaks labeled SB shown in Figure 5A were found to be sidebands.

The resonance at 1.1 ppm which is assigned to ordinary hydride ion was observed in the spectrum of the *KH** sample as shown in Figure 5A. The distinct 0.8 and 1.1 ppm resonances could not be resolved if they were present. A large distinct upfield resonance was observed at -2.8 ppm which was not observed in the control. This upfield shifted peak is assigned to a novel hydride ion of *KH**.

F. NMR of Rubidium Fluoro Hydride Sample

The ^1H MAS NMR spectra of three *RbH*F* samples from separate syntheses, the control comprising an equal molar mixture of *RbH* and *RbF*, and the control *RbH* relative to external tetramethylsilane (TMS) are shown in Figures 6A-E, respectively. Ordinary hydride ion has a resonance at about 1 ppm in the *RbH/ RbF* mixture and in *RbH* alone as shown in Figures 6D and 6E, respectively. The broad peaks at 4 ppm and 4.6 ppm shown in Figures 6D and 6E, respectively, are assigned to *RbOH* formed from air exposure of *RbH* during sample handling. The spin speed was varied to confirm real peaks versus side bands. The latter changed position with spin speed, the former were independent of spin speed. The SB labeled peaks shown in Figure 6D were found to be sidebands.

The presence of *RbF* does not shift the resonance of ordinary hydride. The resonance at 1.2 ppm which is assigned to ordinary hydride ion was observed in the spectrum of each *RbH*F* sample as shown in Figures 6A-C. A large distinct upfield resonance was observed in each case at -4.1 and -4.4 ppm which was not observed in either control. The upfield peak in each sample is assigned to a novel hydride ion of *RbH*F*.

G. NMR of Rubidium Iodo Hydride Sample

The ^1H MAS NMR spectra of two *RbH*I* samples from separate syntheses and the control comprising *RbH* relative to external tetramethylsilane (TMS) are shown in Figures 7A-C, respectively. Ordinary hydride ion has a resonance at about 1 ppm in *RbH* alone as shown in Figure 7C. The broad peaks at 4 ppm shown in Figures 7A-C are assigned to *RbOH* formed from air exposure of *RbH* during sample

handling. The peak at 6 ppm shown in Figures 7A-B are assigned to $RbHCO_3$ formed from air exposure of RbH during sample handling.

The resonance at 1.2 ppm which is assigned to ordinary hydride ion was observed in the spectrum of each $RbH*I$ sample as shown in Figures 7A-B. A large distinct upfield resonance was observed in each case at -3.7 ppm which was not observed in either control. The upfield peak in each sample is assigned to a novel hydride ion of $RbH*I$.

H. NMR of Calcium Hydride Sample

The ^1H MAS NMR spectra of the CaH_2^* sample and control CaH_2 relative to external tetramethylsilane (TMS) are shown in Figures 8A and 8B, respectively. The spin speed was varied to confirm real peaks versus side bands. The latter changed position with spin speed, the former were independent of spin speed. The peaks labeled SB shown in Figures 8A and 8B were found to be sidebands. Resonances at 1.2 ppm and 4.4 ppm were observed in ordinary CaH_2 as shown in Figure 8B.

Three distinct resonances were observed in the case of the CaH_2^* sample at 5.4 ppm, 1.2 ppm, and -1.2 ppm as shown in Figure 8A. The large distinct upfield resonance observed at -1.2 ppm which was not observed in the control is assigned to a novel hydride ion of CaH_2^*.

CONCLUSIONS

The NMR results confirm the identification of novel hydride compounds $MH*X$ wherein M is the metal, X, is a halide, and $H*$ comprises a novel high binding energy hydride ion. Large distinct upfield resonances were observed at -4.5 ppm ($KH*Cl$), -4.1 ppm ($KH*Br$), -3.2 ppm ($KH*I$), -4.4 ppm ($RbH*F$), and -3.7 ppm ($RbH*I$). The presence of a halide in each compound $MH*X$ does not explain the upfield shifted NMR peak since the same NMR spectrum was observed for an equimolar mixture of the pure hydride and the corresponding alkali halide (MH/MX) as was observed for the pure hydride, MH.

The NMR results further confirm the identification of novel hydride compounds $MH*$ and MH_2^* wherein M is the metal and $H*$ comprises a

novel high binding energy hydride ion. Large distinct upfield resonances were observed at -2.8 ppm and -1.2 ppm in the case of $KH*$ and CaH_2^*, respectively. Whereas, the resonances for the ordinary hydride ion of KH were observed at 0.7 and 1.1 ppm, and the resonances for the ordinary hydride ion of CaH_2 were observed at 1.2 ppm and 4.4 ppm. The synthesis of alkaline and alkaline earth hydrides, $KH*$ and CaH_2^*, respectively, with upfield shifted peaks prove that the hydride ion is different from the hydride ion of the corresponding known compound of the same composition.

The upfield shifted peak observed in each novel hydride sample identifies a hydride ion with a smaller radius as compared with ordinary hydride since a smaller radius increases the shielding or diamagnetism. The peaks are assigned to novel hydride ions that have substantially smaller radii than that of ordinary hydride ion since the shift was extraordinarily far upfield. The reproducibility of the syntheses and the results from independent laboratories confirm the formation of novel hydride ions.

The identification of compounds containing novel hydride ions is indicative of a new field of hydrogen chemistry. Novel hydride ions may combine with other cations such as other alkali cations and alkaline earth, rare earth, and transition element cations. Numerous novel compounds may be synthesized with extraordinary properties relative to the corresponding compounds having ordinary hydride ions. These novel compounds may have a breath of applications. For example, a high voltage battery according to the hydride binding energies previously observed by XPS [18-19, 21] may be possible having projected specifications that are comparable to those of the internal combustion engine [19]. An exemplary redox reaction is given in the Appendix.

APPENDIX

Mills [1] predicts that certain atoms or ions serve as catalysts to release energy from hydrogen to produce an increased binding energy hydrogen atom called a *hydrino atom* having a binding energy of

$$Binding\ Energy = \frac{13.6\ eV}{n^2} \tag{1}$$

where

$$n = \frac{1}{2}, \frac{1}{3}, \frac{1}{4}, \ldots, \frac{1}{p} \tag{2}$$

and p is an integer greater than 1, designated as $H\left[\frac{a_H}{p}\right]$ where a_H is the radius of the hydrogen atom. Hydrinos are predicted to form by reacting an ordinary hydrogen atom with a catalyst having a net enthalpy of reaction of about

$$m \cdot 27.2\ eV \tag{3}$$

where m is an integer. This catalysis releases energy from the hydrogen atom with a commensurate decrease in size of the hydrogen atom, $r_n = na_H$. For example, the catalysis of $H(n=1)$ to $H(n=1/2)$ releases $40.8\ eV$, and the hydrogen radius decreases from a_H to $\frac{1}{2}a_H$.

The excited energy states of atomic hydrogen are also given by Eq. (1) except that

$$n = 1, 2, 3, \ldots \tag{4}$$

The $n=1$ state is the "ground" state for "pure" photon transitions (the $n=1$ state can absorb a photon and go to an excited electronic state, but it cannot release a photon and go to a lower-energy electronic state). However, an electron transition from the ground state to a lower-energy state is possible by a nonradiative energy transfer such as multipole coupling or a resonant collision mechanism. These lower-energy states have fractional quantum numbers, $n = \frac{1}{\text{integer}}$. Processes that occur without photons and that require collisions are common. For example, the exothermic chemical reaction of $H + H$ to form H_2 does not occur with the emission of a photon. Rather, the reaction requires a collision with a third body, M, to remove the bond energy- $H + H + M \rightarrow H_2 + M^*$ [34]. The third body distributes the energy from the exothermic reaction, and the end result is the H_2 molecule and an increase in the temperature of the system. Some commercial phosphors are based on nonradiative energy transfer involving multipole coupling. For example, the strong absorption strength of Sb^{3+} ions along with the efficient nonradiative transfer of excitation from Sb^{3+} to Mn^{2+}, are responsible for the strong manganese luminescence from phosphors containing these ions [35]. Similarly, the

$n=1$ state of hydrogen and the $n=\frac{1}{\text{integer}}$ states of hydrogen are nonradiative, but a transition between two nonradiative states is possible via a nonradiative energy transfer, say $n=1$ to $n=1/2$. In these cases, during the transition the electron couples to another electron transition, electron transfer reaction, or inelastic scattering reaction which can absorb the exact amount of energy that must be removed from the hydrogen atom. Thus, a catalyst provides a net positive enthalpy of reaction of $m \cdot 27.2\,eV$ (i.e. it absorbs $m \cdot 27.2\,eV$ where m is an integer). Certain atoms or ions serve as catalysts which resonantly accept energy from hydrogen atoms and release the energy to the surroundings to effect electronic transitions to fractional quantum energy levels.

Inorganic Catalysts

Potassium

A catalytic system is provided by the ionization of t electrons from an atom to a continuum energy level such that the sum of the ionization energies of the t electrons is approximately $m\,X\,27.2\,eV$ where m is an integer. One such catalytic system involves potassium. A catalytic system is provided by the ionization of 3 electrons from a potassium atom each to a continuum energy level such that the sum of the ionization energies of the 3 electrons is approximately $3 \cdot 27.2\,eV$. The first, second, and third ionization energies of potassium are $4.34066\,eV$, $31.63\,eV$, $45.806\,eV$, respectively [32]. The triple ionization ($t=3$) reaction of K to K^{3+}, then, has a net enthalpy of reaction of $81.7426\,eV$, which is equivalent to $m=3$ in Eq. (3).

$$81.7426\,eV + K(m) + H\left[\frac{a_H}{p}\right] \rightarrow K^{3+} + 3e^- + H\left[\frac{a_H}{(p+3)}\right] + [(p+3)^2 - p^2]X13.6\,eV \qquad (5)$$

$$K^{3+} + 3e^- \rightarrow K(m) + 81.7426\,eV \qquad (6)$$

And, the overall reaction is

$$H\left[\frac{a_H}{p}\right] \rightarrow H\left[\frac{a_H}{(p+3)}\right] + [(p+3)^2 - p^2]X13.6\ eV \tag{7}$$

Potassium ions can also provide a net enthalpy of a multiple of that of the potential energy of the hydrogen atom. The second ionization energy of potassium is $31.63\ eV$; and K^+ releases $4.34\ eV$ when it is reduced to K [32]. The combination of reactions K^+ to K^{2+} and K^+ to K, then, has a net enthalpy of reaction of $27.28\ eV$, which is equivalent to $m=1$ in Eq. (3).

$$27.28\ eV + K^+ + K^+ + H\left[\frac{a_H}{p}\right] \rightarrow K + K^{2+} + H\left[\frac{a_H}{(p+1)}\right] + [(p+1)^2 - p^2]\ X\ 13.6\ eV \tag{8}$$

$$K + K^{2+} \rightarrow K^+ + K^+ + 27.28\ eV \tag{9}$$

The overall reaction is

$$H\left[\frac{a_H}{p}\right] \rightarrow H\left[\frac{a_H}{(p+1)}\right] + [(p+1)^2 - p^2]\ X\ 13.6\ eV \tag{10}$$

Rubidium

Rubidium ions can also provide a net enthalpy of a multiple of that of the potential energy of the hydrogen atom. A catalytic system is provided by the ionization of an electron from a Rb^+ ion to a continuum energy level since the second ionization energy of rubidium is $27.28\ eV$ [32]. The reaction Rb^+ to Rb^{2+} has a net enthalpy of reaction of $27.28\ eV$, which is equivalent to $m=1$ in Eq. (3).

$$27.28\ eV + Rb^+ + H\left[\frac{a_H}{p}\right] \rightarrow Rb^{2+} + e^- + H\left[\frac{a_H}{(p+1)}\right] + [(p+1)^2 - p^2]X13.6\ eV \tag{12}$$

$$Rb^{2+} + e^- \rightarrow Rb^+ + 27.28\ eV \tag{12}$$

The overall reaction is

$$H\left[\frac{a_H}{p}\right] \rightarrow H\left[\frac{a_H}{(p+1)}\right] + [(p+1)^2 - p^2]\ X\ 13.6\ eV \tag{13}$$

Hydride Ion

A novel hydride ion having extraordinary chemical properties given by Mills [1] is predicted to form by the reaction of an electron with a hydrino (Eq. (14)). The resulting hydride ion is referred to as a hydrino hydride ion, designated as $H^-(1/p)$.

$$H\left[\frac{a_H}{p}\right]+e^- \rightarrow H^-(1/p) \tag{14}$$

The hydrino hydride ion is distinguished from an ordinary hydride ion having a binding energy of 0.8 eV. The hydrino hydride ion is predicted [1] to comprise a hydrogen nucleus and two indistinguishable electrons at a binding energy according to the following formula:

$$Binding\ Energy = \frac{\hbar^2\sqrt{s(s+1)}}{8\mu_e a_0^2\left[\frac{1+\sqrt{s(s+1)}}{p}\right]^2} - \frac{\pi\mu_0 e^2\hbar^2}{m_e^2 a_0^3}\left(1+\frac{2^2}{\left[\frac{1+\sqrt{s(s+1)}}{p}\right]^3}\right) \tag{15}$$

where p is an integer greater than one, $s=1/2$, π is pi, $\hbar$ is Planck's constant bar, μ_o is the permeability of vacuum, m_e is the mass of the electron, μ_e is the reduced electron mass, a_o is the Bohr radius, and e is the elementary charge. The ionic radius is

$$r_1 = \frac{a_0}{p}\left(1+\sqrt{s(s+1)}\right);\ s=\frac{1}{2} \tag{16}$$

From Eq. (16), the radius of the hydrino hydride ion $H^-(1/p);\ p=\text{integer}$ is $\frac{1}{p}$ that of ordinary hydride ion, $H^-(1/1)$. Compounds containing hydrino hydride ions have been isolated as products of the reaction of atomic hydrogen with atoms and ions identified as catalysts by EUV emission [2-31].

Hydride ions having extraordinary binding energies may stabilize a cation M^{x+} in an extraordinarily high oxidation state such as +2 in the case of lithium. Thus, these hydride ions may be used as the basis of a

high voltage battery of a rocking chair design wherein the hydride ion moves back and forth between the cathode and anode half cells during discharge and charge cycles. Exemplary reactions for a cation M^{x+} are:

Cathode reaction:

$$MH_x + e^- \rightarrow MH_{x-1} + H^- \quad (17)$$

Anode reaction:

$$MH_{x-2} + H^- \rightarrow MH_{x-1} + e^- \quad (18)$$

Overall reaction:

$$MH_x + MH_{x-2} \rightarrow 2MH_{x-1} \quad (19)$$

REFERENCES

1. R. Mills, The Grand Unified Theory of Classical Quantum Mechanics, January 2000 Edition, BlackLight Power, Inc., Cranbury, New Jersey, Distributed by Amazon.com.
2. R. Mills and M. Nansteel, "Anomalous Argon-Hydrogen-Strontium Discharge", IEEE Transactions of Plasma Science, submitted.
3. R. Mills, M. Nansteel, and Y. Lu, "Anomalous Hydrogen-Strontium Discharge", European Journal of Physics D, submitted.
4. R. Mills, "Spectroscopic Identification of a Novel Catalytic Reaction of Atomic Hydrogen and the Hydride Ion Product", Int. J. Hydrogen Energy, submitted.
5. R. Mills, N. Greenig, S. Hicks, "Optically Measured Power Balances of Anomalous Discharges of Mixtures of Argon, Hydrogen, and Potassium, Rubidium, Cesium, or Strontium Vapor", Int. J. Hydrogen Energy, submitted.
6. R. Mills, J. Dong, Y. Lu, "Observation of Extreme Ultraviolet Hydrogen Emission from Incandescently Heated Hydrogen Gas with Certain Catalysts", Int. J. Hydrogen Energy, Vol. 25, (2000), pp. 919-943.
7. R. Mills, "Observation of Extreme Ultraviolet Emission from Hydrogen-KI Plasmas Produced by a Hollow Cathode Discharge", Int. J. Hydrogen Energy, in press.
8. R. Mills, "Temporal Behavior of Light-Emission in the Visible Spectral Range from a Ti-K2CO3-H-Cell", Int. J. Hydrogen Energy, in press.
9. R. Mills, Y. Lu, and T. Onuma, "Formation of a Hydrogen Plasma from an Incandescently Heated Hydrogen-Catalyst Gas Mixture with an Anomalous Afterglow Duration", Int. J. Hydrogen Energy, in press.
10. R. Mills, M. Nansteel, and Y. Lu, "Observation of Extreme Ultraviolet Hydrogen Emission from Incandescently Heated Hydrogen Gas with Strontium that Produced an Anomalous Optically Measured Power Balance", Int. J. Hydrogen Energy, in press.
11. R. Mills, J. Dong, Y. Lu, J. Conrads, "Observation of Extreme Ultraviolet Hydrogen Emission from Incandescently Heated Hydrogen Gas with Certain Catalysts", 1999 Pacific Conference on Chemistry and Spectroscopy and the 35th ACS Western Regional Meeting, Ontario Convention Center, California, (October 6-8, 1999).

12. R. Mills, J. Dong, N. Greenig, and Y. Lu, "Observation of Extreme Ultraviolet Hydrogen Emission from Incandescently Heated Hydrogen Gas with Certain Catalysts", National Hydrogen Association, 11 th Annual U.S. Hydrogen Meeting, Vienna, VA, (February 29-March 2, 2000).
13. R. Mills, B. Dhandapani, N. Greenig, J. He, J. Dong, Y. Lu, and H. Conrads, "Formation of an Energetic Plasma and Novel Hydrides from Incandescently Heated Hydrogen Gas with Certain Catalysts", National Hydrogen Association, 11 th Annual U.S. Hydrogen Meeting, Vienna, VA, (February 29-March 2, 2000).
14. Mills, J. Dong, N. Greenig, and Y. Lu, "Observation of Extreme Ultraviolet Hydrogen Emission from Incandescently Heated Hydrogen Gas with Certain Catalysts", 219 th National ACS Meeting, San Francisco, California, (March 26-30, 2000).
15. R. Mills, B. Dhandapani, N. Greenig, J. He, J. Dong, Y. Lu, and H. Conrads, "Formation of an Energetic Plasma and Novel Hydrides from Incandescently Heated Hydrogen Gas with Certain Catalysts", 219 th National ACS Meeting, San Francisco, California, (March 26-30, 2000).
16. R. Mills, B. Dhandapani, N. Greenig, J. He, J. Dong, Y. Lu, and H. Conrads, "Formation of an Energetic Plasma and Novel Hydrides from Incandescently Heated Hydrogen Gas with Certain Catalysts", June ACS Meeting (29th Northeast Regional Meeting, University of Connecticut, Storrs, CT, (June 18-21, 2000)).
17. R. Mills, B. Dhandapani, N. Greenig, J. He, J. Dong, Y. Lu, and H. Conrads, "Formation of an Energetic Plasma and Novel Hydrides from Incandescently Heated Hydrogen Gas with Certain Catalysts", August National ACS Meeting (220th ACS National Meeting, Washington, DC, (August 20-24, 2000)).
18. R. Mills, B. Dhandapani, N. Greenig, J. He, "Synthesis and Characterization of Potassium Iodo Hydride", Int. J. of Hydrogen Energy, Vol. 25, Issue 12, December, (2000), pp. 1185-1203.
19. R. Mills, "Novel Inorganic Hydride", Int. J. of Hydrogen Energy, Vol. 25, (2000), pp. 669-683.
20. R. Mills, "Novel Hydrogen Compounds from a Potassium Carbonate Electrolytic Cell", Fusion Technology, Vol. 37, No. 2, March, (2000), pp. 157-182.

21. R. Mills, B. Dhandapani, M. Nansteel, J. He, T. Shannon, A. Echezuria, "Synthesis and Characterization of Novel Hydride Compounds", Int. J. of Hydrogen Energy, in press.
22. R. Mills, "Highly Stable Novel Inorganic Hydrides", Journal of Materials Research, submitted.
23. R. Mills, "Novel Hydride Compound", 1999 Pacific Conference on Chemistry and Spectroscopy and the 35th ACS Western Regional Meeting, Ontario Convention Center, California, (October 6-8, 1999).
24. R. Mills, B, Dhandapani, N. Greenig, J. He, "Synthesis and Characterization of Potassium Iodo Hydride", 1999 Pacific Conference on Chemistry and Spectroscopy and the 35th ACS Western Regional Meeting, Ontario Convention Center, California, (October 6-8, 1999).
25. R. Mills, J. He, and B. Dhandapani, "Novel Hydrogen Compounds", 1999 Pacific Conference on Chemistry and Spectroscopy and the 35th ACS Western Regional Meeting, Ontario Convention Center, California, (October 6-8, 1999).
26. R. Mills, "Novel Hydride Compound", National Hydrogen Association, 11 th Annual U.S. Hydrogen Meeting, Vienna, VA, (February 29-March 2, 2000).
27. R. Mills, J. He, and B. Dhandapani, "Novel Alkali and Alkaline Earth Hydrides", National Hydrogen Association, 11 th Annual U.S. Hydrogen Meeting, Vienna, VA, (February 29-March 2, 2000).
28. R. Mills, "Novel Hydride Compound", 219 th National ACS Meeting, San Francisco, California, (March 26-30, 2000).
29. R. Mills, J. He, and B. Dhandapani, "Novel Alkali and Alkaline Earth Hydrides", 219 th National ACS Meeting, San Francisco, California, (March 26-30, 2000).
30. R. Mills, J. He, and B. Dhandapani, "Novel Alkali and Alkaline Earth Hydrides", August National ACS Meeting (220 th ACS National Meeting, Washington, DC, (August 20-24, 2000)).
31. R. Mills, W. Good, A. Voigt, Jinquan Dong, "Minimum Heat of Formation of Potassium Iodo Hydride", Int. J. Hydrogen Energy, submitted.
32. David R. Linde, *CRC Handbook of Chemistry and Physics*, 79 th Edition, CRC Press, Boca Raton, Florida, (1998-9), p. 10-175 to p. 10-177.

33. R. Mills, The Nature of Free Electrons in Superfluid Helium--a Test of Quantum Mechanics and a Basis to Review its Foundations and Make a Comparison to Classical Theory, Int. J. Hydrogen Energy, in press.
34. N. V. Sidgwick, *The Chemical Elements and Their Compounds*, Volume I, Oxford, Clarendon Press, (1950), p.17.
35. M. D. Lamb, *Luminescence Spectroscopy*, Academic Press, London, (1978), p. 68.

Table 1. Comparison of solid-state ^1H MAS NMR spectral data of $KH*Cl$ and $KH*I$ from various analytical laboratories.

Sample	Laboratory	Novel features
$KH*Cl$	Spectral Data Services	-4.6 ppm
$KH*Cl$	University of Massachusetts	-4.4 ppm
$KH*Cl$	University of Delaware	-4.9 ppm
$KH*Cl$	Grace Davison	-4.5 ppm
$KH*I$ (blue crystals)	Spectral Data Services	-1.8 ppm
$KH*I$ (green crystals)	Spectral Data Services	-2.6 ppm
$KH*I$ (blue crystals)	National Research Council of Canada	-1.2 ppm -2.5 ppm[a]
$KH*I$ (blue crystals)	Grace Davison	-1.5 ppm -2.3 ppm[a]
$KH*I$ (green crystals)	University of Delaware	-2.8 ppm

[a] (smaller peak)

Figure Captions

Figure 1. Stainless steel gas cell comprising a screen dissociator, metal catalyst, and alkali halide or alkali or alkaline earth hydride as the reactant. The components were: 101-stainless steel cell; 117- internal cavity of cell; 118-high vacuum conflat flange; 119-mating blank conflat flange; 102-stainless steel tube vacuum line and gas supply line; 103-lid to the kiln or top insulation, 104 heater; 108-screen dissociator; 109-alkali halide or alkali or alkaline earth hydride reactant; 110-high vacuum turbo pump; 112- pressure gauge; 111-vacuum pump valve; 113-valve; 114-valve; 115-regulator; 116-hydrogen tank.

Figure 2A-F. The ^1H MAS NMR spectra of six $KH*Cl$ samples from independent syntheses relative to external tetramethylsilane (TMS).

Figure 2G. The ^1H MAS NMR spectrum of the control comprising an equal molar mixture of KH and KCl relative to external tetramethylsilane (TMS).

Figure 2H. The ^1H MAS NMR spectrum of the control KH relative to external tetramethylsilane (TMS).

Figure 3A. The ^1H MAS NMR spectrum of $KH*Br$ relative to external tetramethylsilane (TMS).

Figure 3B. The ^1H MAS NMR spectrum of the control comprising an equal molar mixture of KH and KBr relative to external tetramethylsilane (TMS).

Figure 3C. The ^1H MAS NMR spectrum of the control KH relative to external tetramethylsilane (TMS).

Figure 4A. The ^1H MAS NMR spectrum of $KH*I$ (dark green crystals) relative to external tetramethylsilane (TMS).

Figure 4B. The ^1H MAS NMR spectrum of $KH*I$ (green crystals) relative to external tetramethylsilane (TMS).

Figure 4C. The ^1H MAS NMR spectrum of $KH*I$ (blue crystals) relative to external tetramethylsilane (TMS).

Figure 4D. The ^1H MAS NMR spectrum of the control comprising an equal molar mixture of KH and KI relative to external tetramethylsilane (TMS).

Figure 4E. The ^1H MAS NMR spectrum of the control KH relative to external tetramethylsilane (TMS).

Figure 5A. The ^1H MAS NMR spectra of KH^* relative to external tetramethylsilane (TMS).

Figure 5B. The ^1H MAS NMR spectrum of the control KH relative to external tetramethylsilane (TMS).

Figure 6A-C. The ^1H MAS NMR spectra of three RbH^*F samples from separate syntheses relative to external tetramethylsilane (TMS).

Figure 6D. The ^1H MAS NMR spectrum of the control comprising an equal molar mixture of RbH and RbF relative to external tetramethylsilane (TMS).

Figure 6E. The ^1H MAS NMR spectrum of the control RbH relative to external tetramethylsilane (TMS).

Figure 7A-B. The ^1H MAS NMR spectra of two RbH^*I samples from separate syntheses relative to external tetramethylsilane (TMS).

Figure 7C. The ^1H MAS NMR spectrum of the control RbH relative to external tetramethylsilane (TMS).

Figure 8A. The ^1H MAS NMR spectra of the CaH_2^* relative to external tetramethylsilane (TMS).

Figure 8B. The ^1H MAS NMR spectrum of the control CaH_2 relative to external tetramethylsilane (TMS).

Figure 9. The ^1H MAS NMR spectrum of KH^*Cl performed at Spectral Data Services relative to external tetramethylsilane (TMS).

Figure 10. The ^1H MAS NMR spectrum of KH^*Cl performed at University of Massachusetts relative to external tetramethylsilane (TMS).

Figure 11. The ^1H MAS NMR spectrum of KH^*Cl performed at University of Delaware relative to external tetramethylsilane (TMS).

Figure 12. The ^1H MAS NMR spectrum of KH^*Cl performed at Grace Davison relative to external tetramethylsilane (TMS).

Figure 13. The ^1H MAS NMR spectrum of KH^*I (blue crystals) performed at Spectral Data Services relative to external tetramethylsilane (TMS).

Figure 14. The ^1H MAS NMR spectrum of KH^*I (green crystals) performed at Spectral Data Services relative to external tetramethylsilane (TMS).

Figure 15. The ^1H MAS NMR spectrum of KH^*I (blue crystals) performed at National Research Council of Canada relative to external tetramethylsilane (TMS).

Figure 16. The ^{1}H MAS NMR spectrum of $KH*I$ (blue crystals) performed at Grace Davison relative to external tetramethylsilane (TMS).

Figure 17. The ^{1}H MAS NMR spectrum of $KH*I$ (blue crystals) performed at National University of Delaware relative to external tetramethylsilane (TMS).

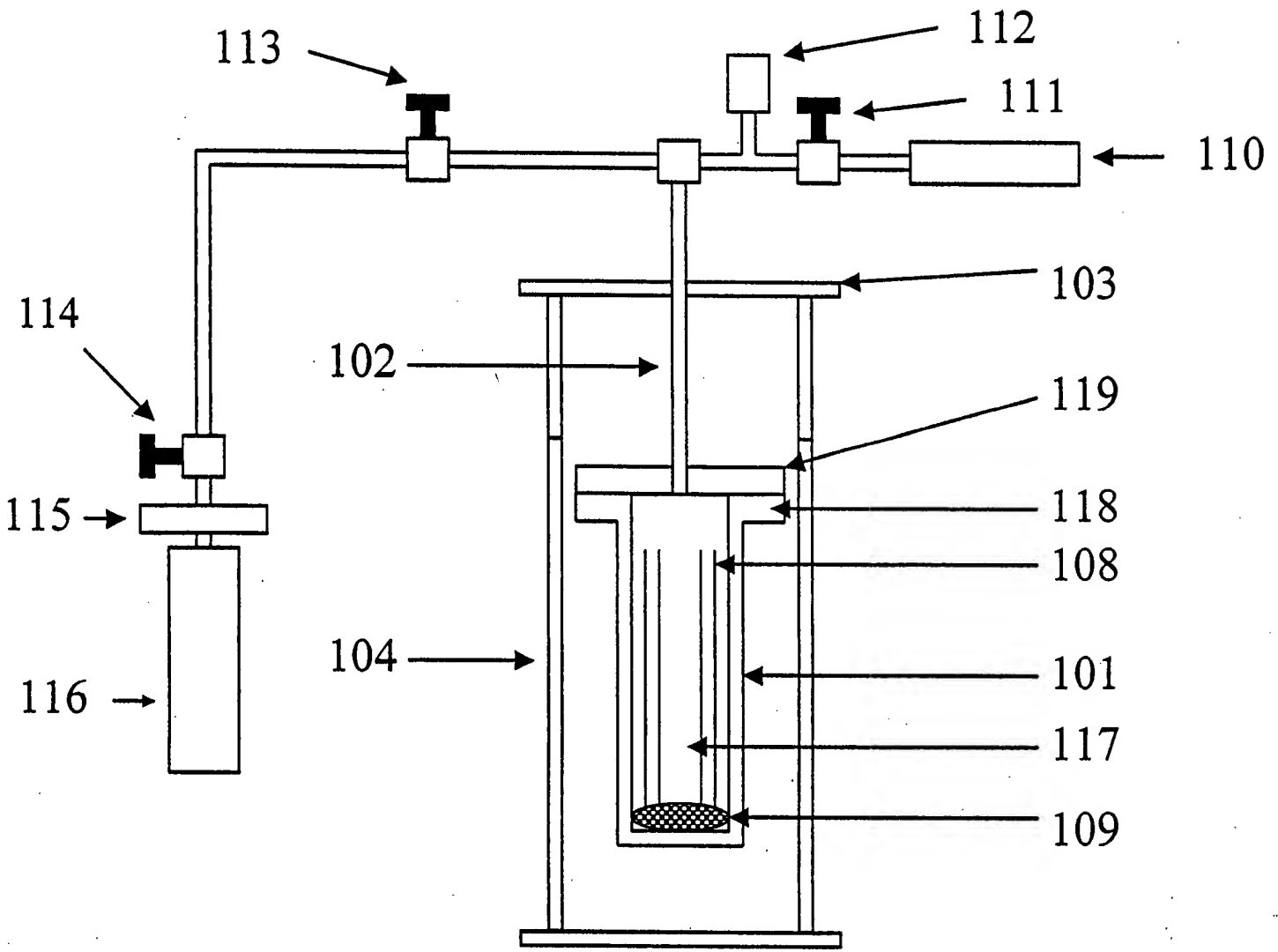

Fig. 1

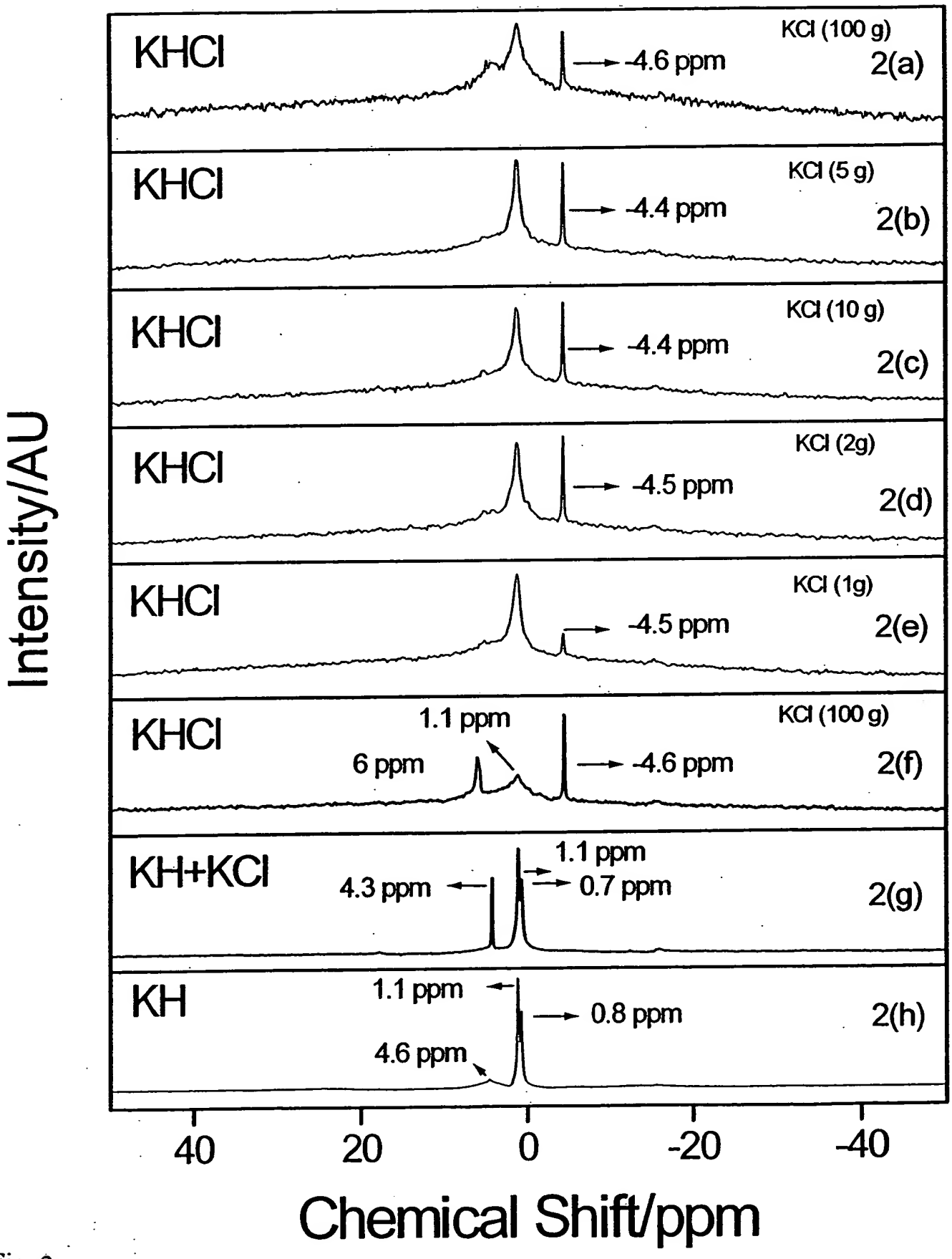
KHCl
KCl (100 g)
-4.6 ppm
2(a)
KHCl
KCl (5 g)
-4.4 ppm
2(b)
KHCl
KCl (10 g)
-4.4 ppm
2(c)
KHCl
KCl (2g)
-4.5 ppm
2(d)
KHCl
KCl (1g)
-4.5 ppm
2(e)
KHCl
1.1 ppm
6 ppm
KCl (100 g)
-4.6 ppm
2(f)
KH+KCl
4.3 ppm
1.1 ppm
0.7 ppm
2(g)
KH
1.1 ppm
4.6 ppm
0.8 ppm
2(h)
Intensity/AU
40
20
0
-20
-40
Chemical Shift/ppm

Fig. 2

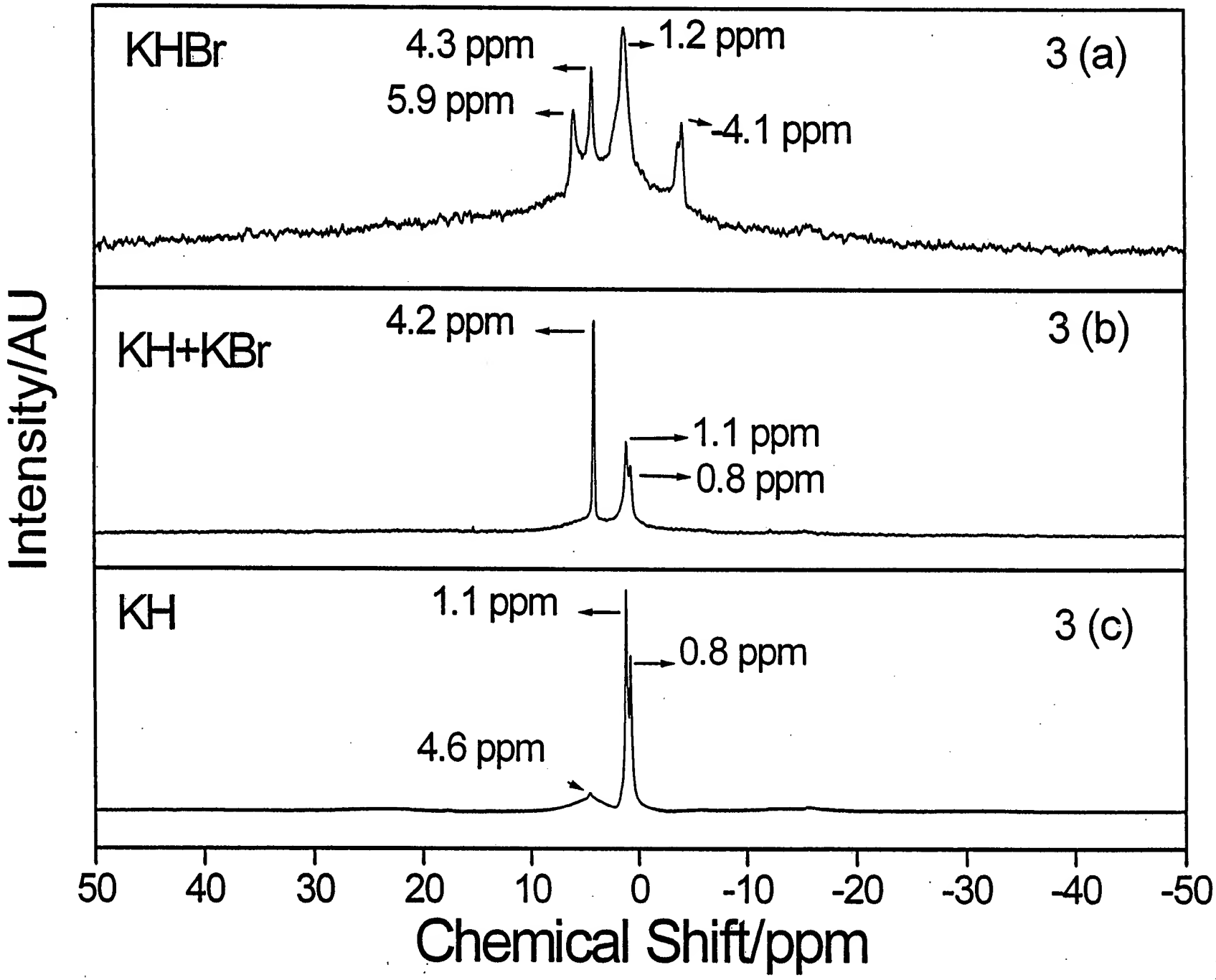
KHBr
4.3 ppm
1.2 ppm
3 (a)
5.9 ppm
4.1 ppm
KH+KBr
4.2 ppm
3 (b)
1.1 ppm
0.8 ppm
KH
1.1 ppm
3 (c)
0.8 ppm
4.6 ppm
Intensity/AU
50
40
30
20
10
0
-10
-20
-30
-40
-50
Chemical Shift/ppm

Fig. 3

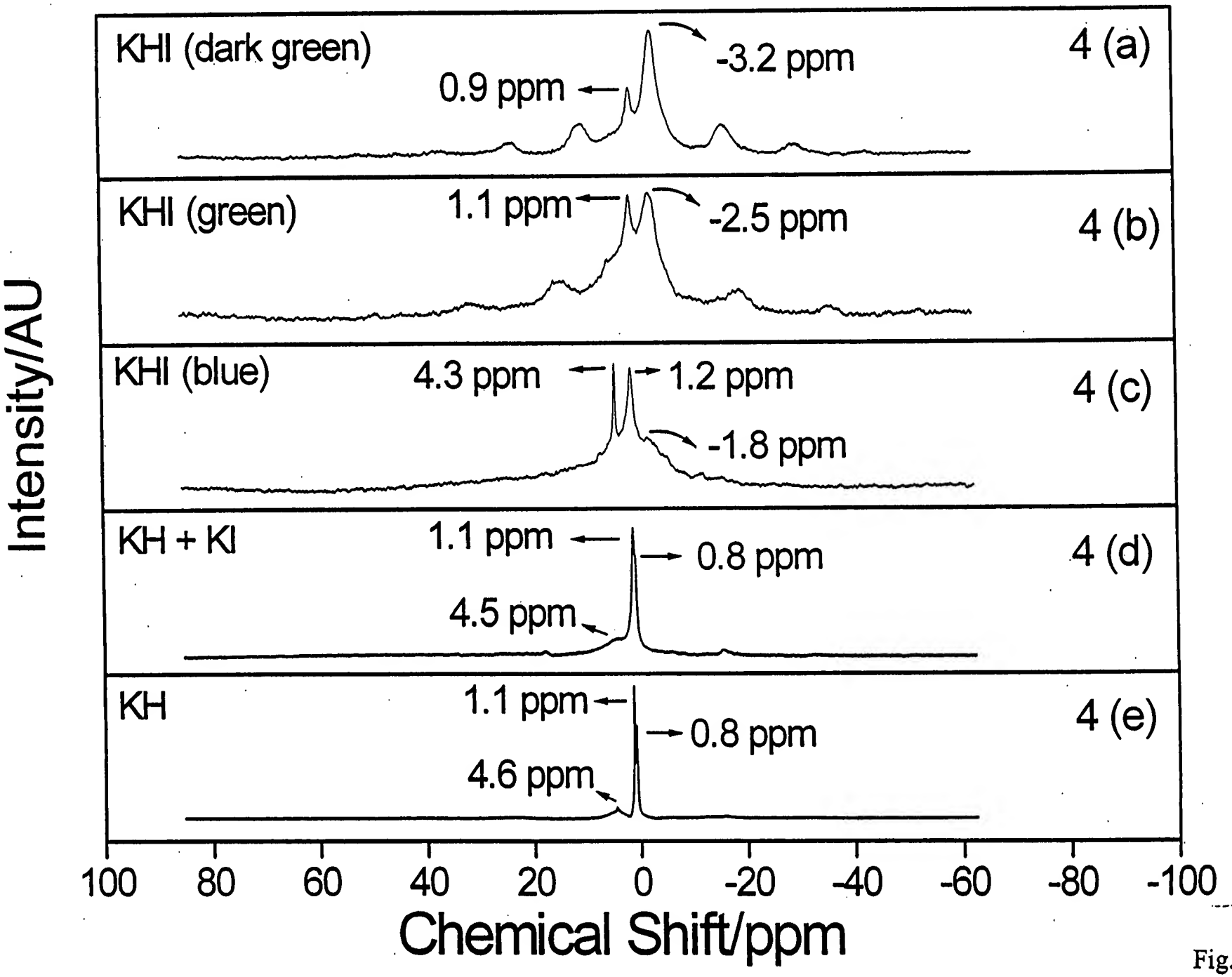
KHI (dark green)
0.9 ppm
-3.2 ppm
4 (a)
KHI (green)
1.1 ppm
-2.5 ppm
4 (b)
KHI (blue)
4.3 ppm
1.2 ppm
-1.8 ppm
4 (c)
KH + KI
1.1 ppm
0.8 ppm
4.5 ppm
4 (d)
KH
1.1 ppm
0.8 ppm
4.6 ppm
4 (e)
Intensity/AU
100
80
60
40
20
0
-20
-40
-60
-80
-100
Chemical Shift/ppm

Fig. 4

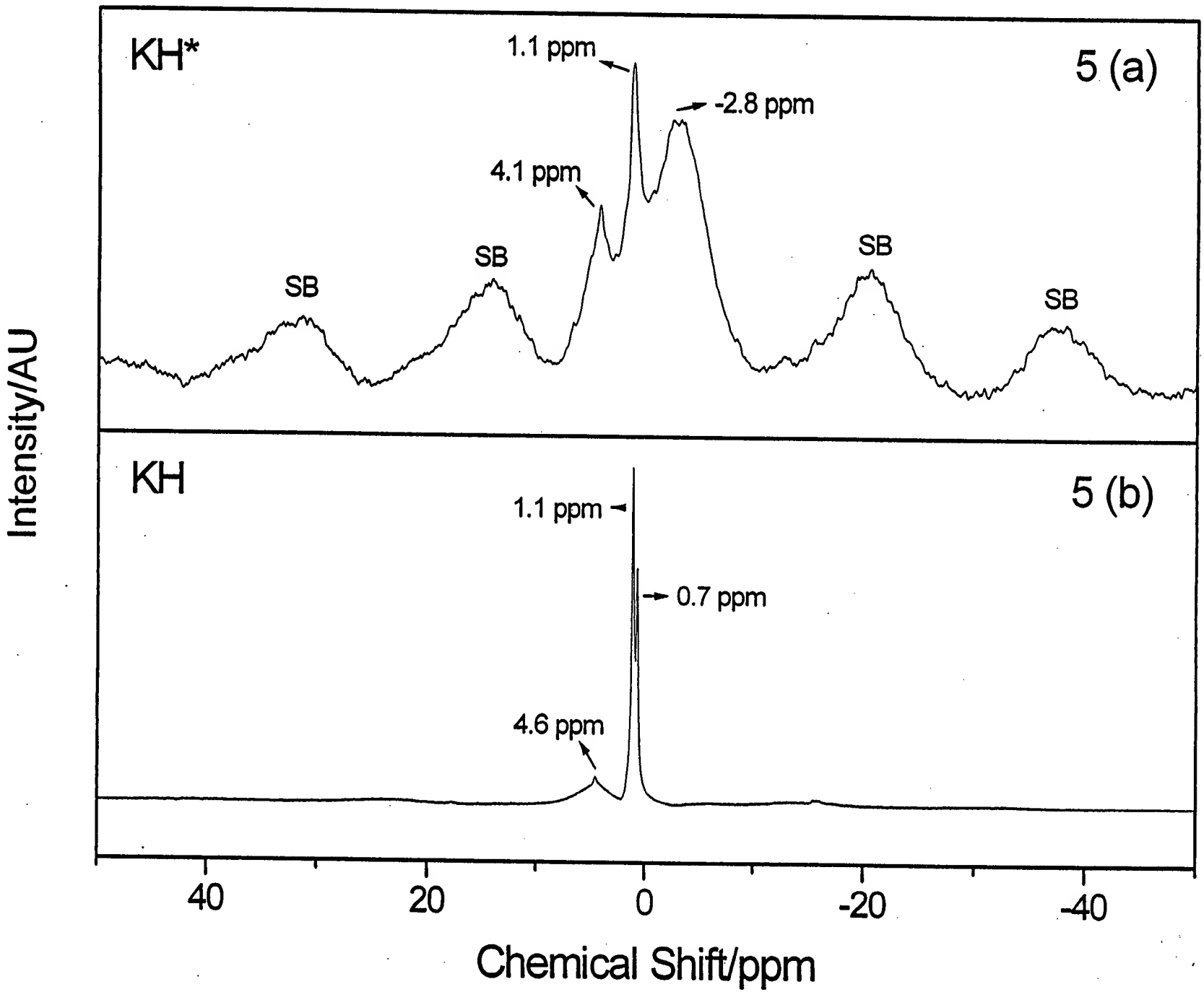
KH*
1.1 ppm
5 (a)
-2.8 ppm
4.1 ppm
SB
SB
SB
SB
KH
1.1 ppm
5 (b)
0.7 ppm
4.6 ppm
Intensity/AU
40
20
0
-20
-40
Chemical Shift/ppm

Fig. 5

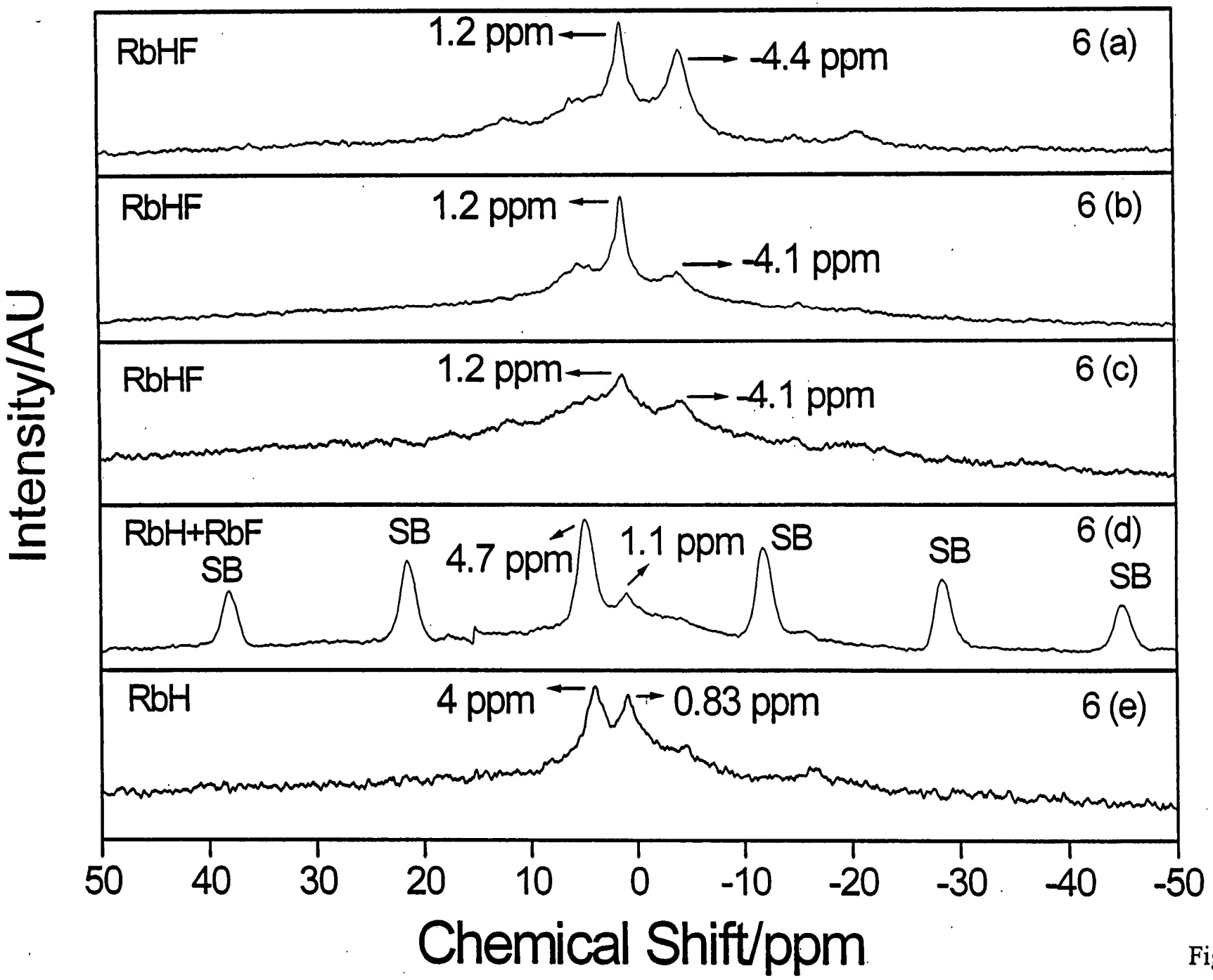
RbHF
1.2 ppm
-4.4 ppm
6 (a)
RbHF
1.2 ppm
-4.1 ppm
6 (b)
RbHF
1.2 ppm
-4.1 ppm
6 (c)
RbH+RbF
SB
SB
4.7 ppm
1.1 ppm
SB
SB
SB
6 (d)
RbH
4 ppm
0.83 ppm
6 (e)
Intensity/AU
50
40
30
20
10
0
-10
-20
-30
-40
-50
Chemical Shift/ppm

Fig. 6

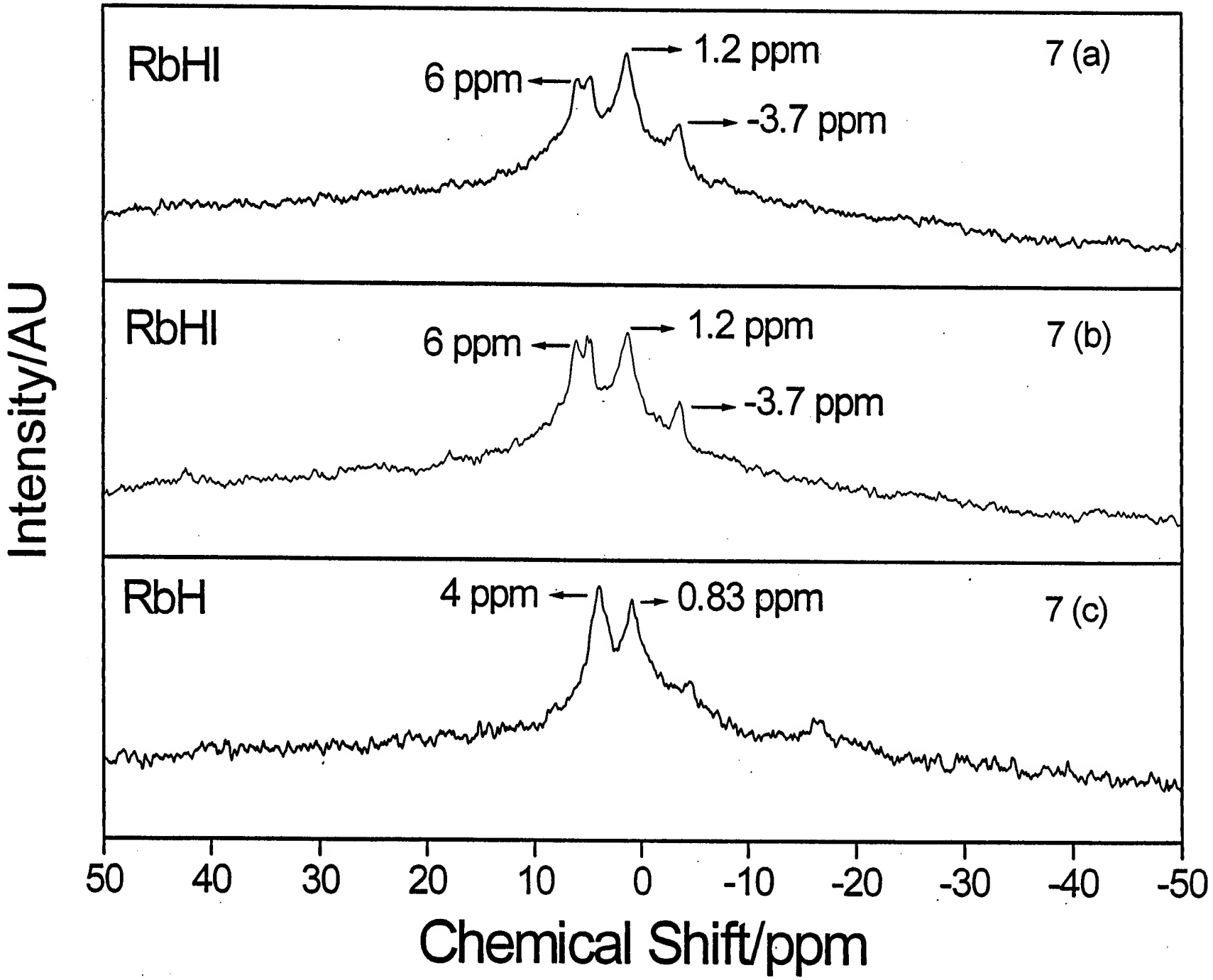
RbHI
6 ppm
1.2 ppm
-3.7 ppm
7 (a)
RbHI
6 ppm
1.2 ppm
-3.7 ppm
7 (b)
RbH
4 ppm
0.83 ppm
7 (c)
Intensity/AU
50
40
30
20
10
0
-10
-20
-30
-40
-50
Chemical Shift/ppm

Fig. 7

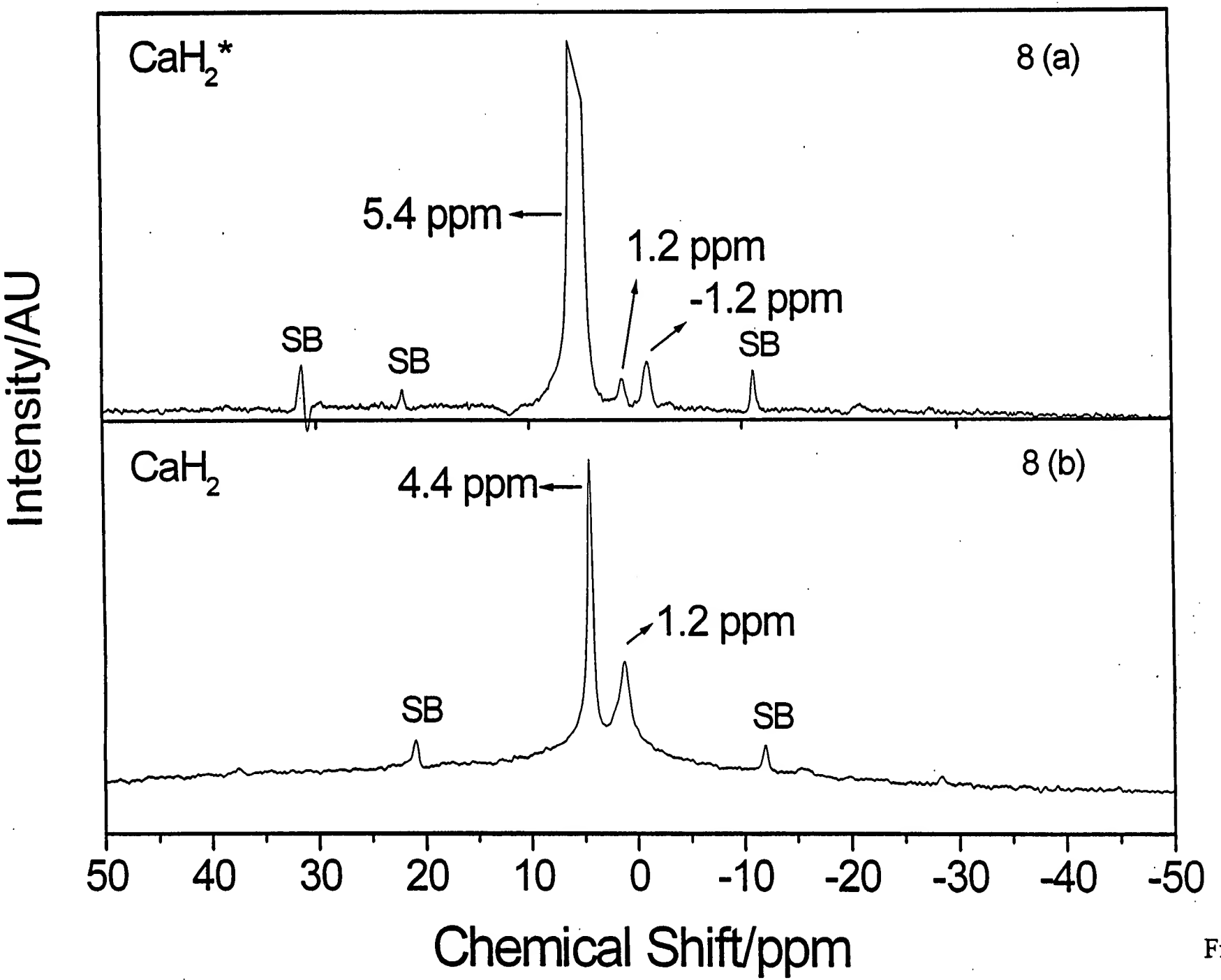
CaH2*
8 (a)
5.4 ppm
1.2 ppm
-1.2 ppm
SB
SB
SB
CaH2
8 (b)
4.4 ppm
1.2 ppm
SB
SB
Intensity/AU
50
40
30
20
10
0
-10
-20
-30
-40
-50
Chemical Shift/ppm

Fig. 8

Fig. 9

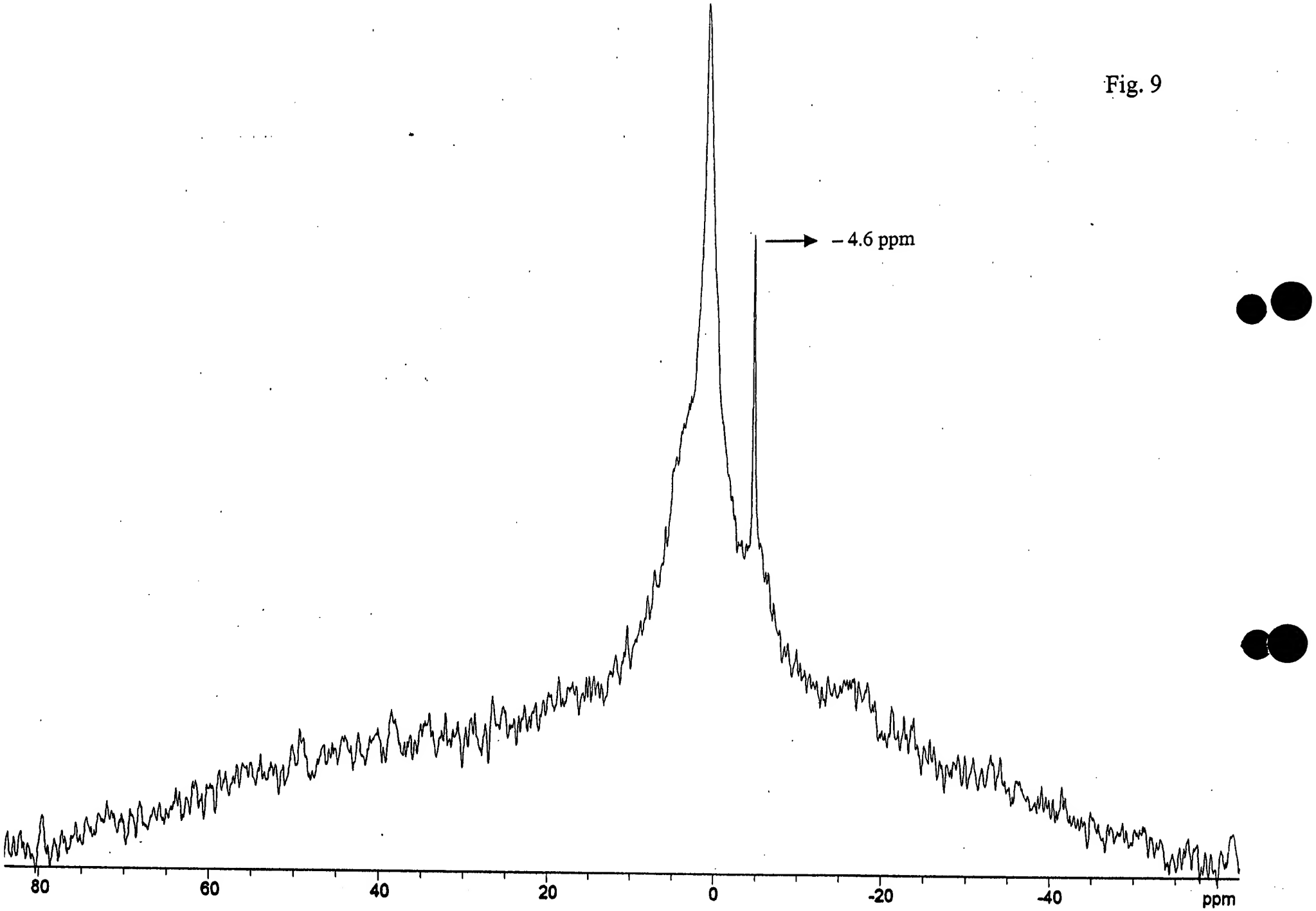

Fig. 10

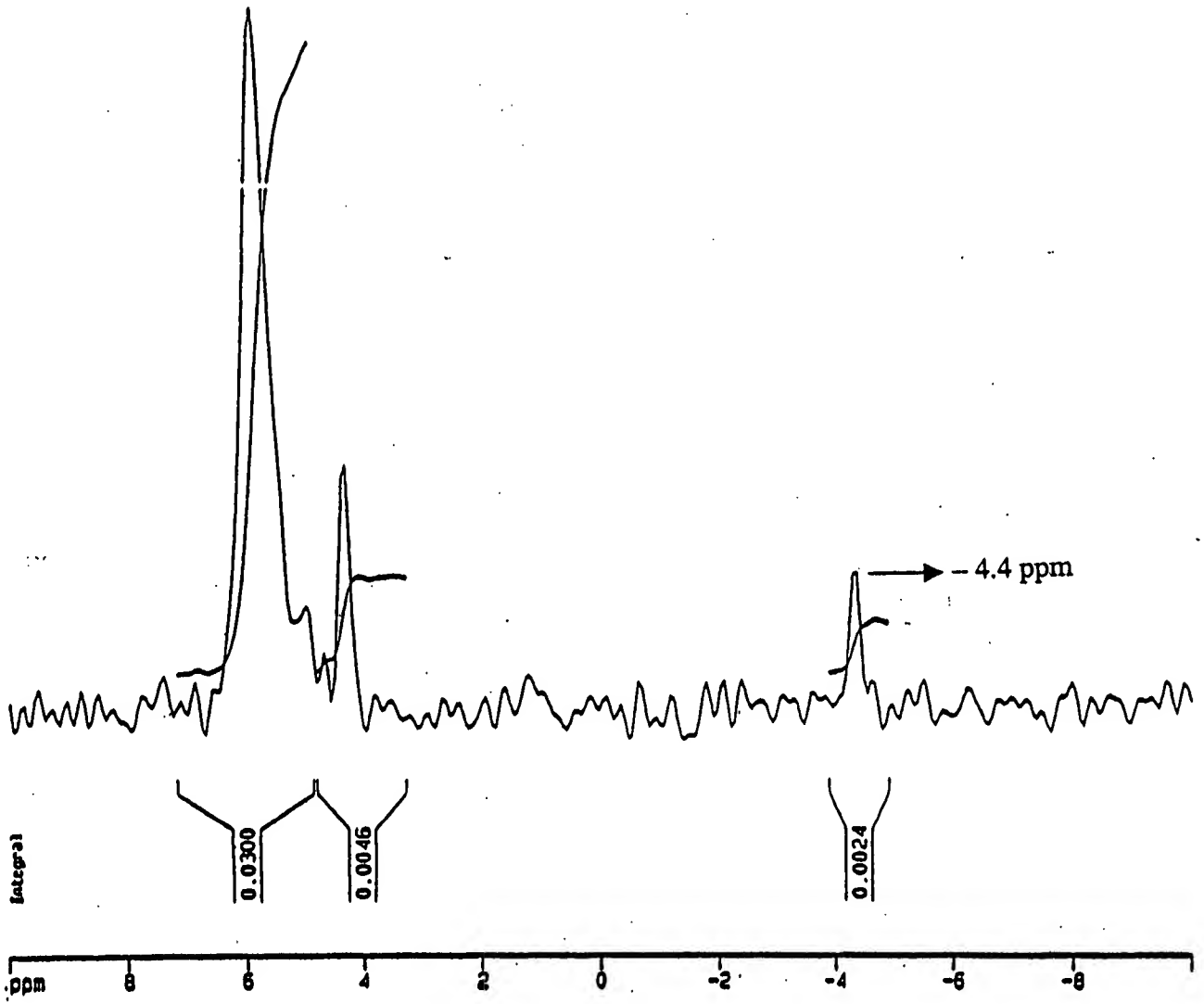

Fig. 11

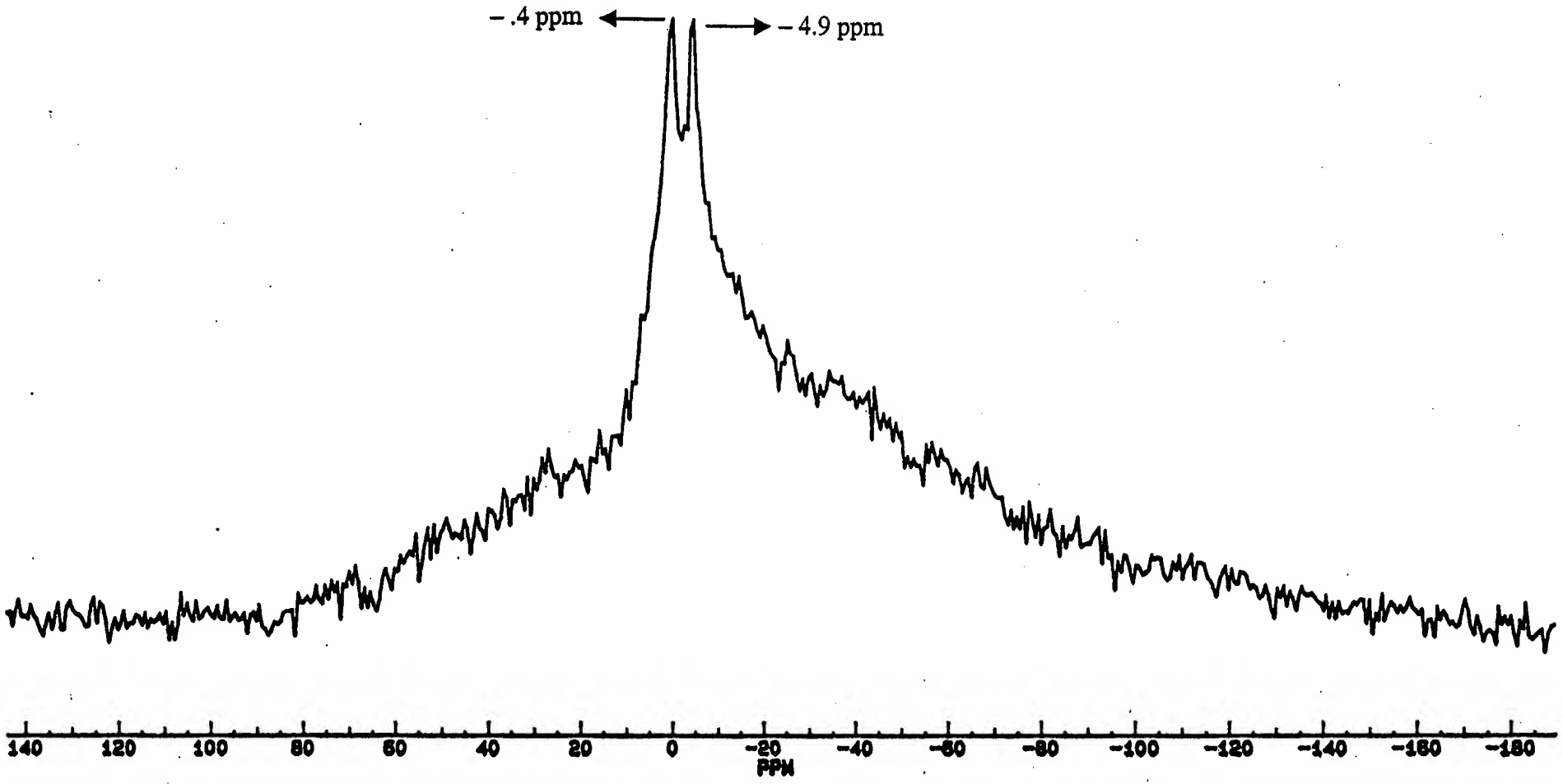
– .4 ppm
– 4.9 ppm
140
120
100
80
60
40
20
0
-20
-40
-60
-80
-100
-120
-140
-160
-180
PPM

Fig. 12

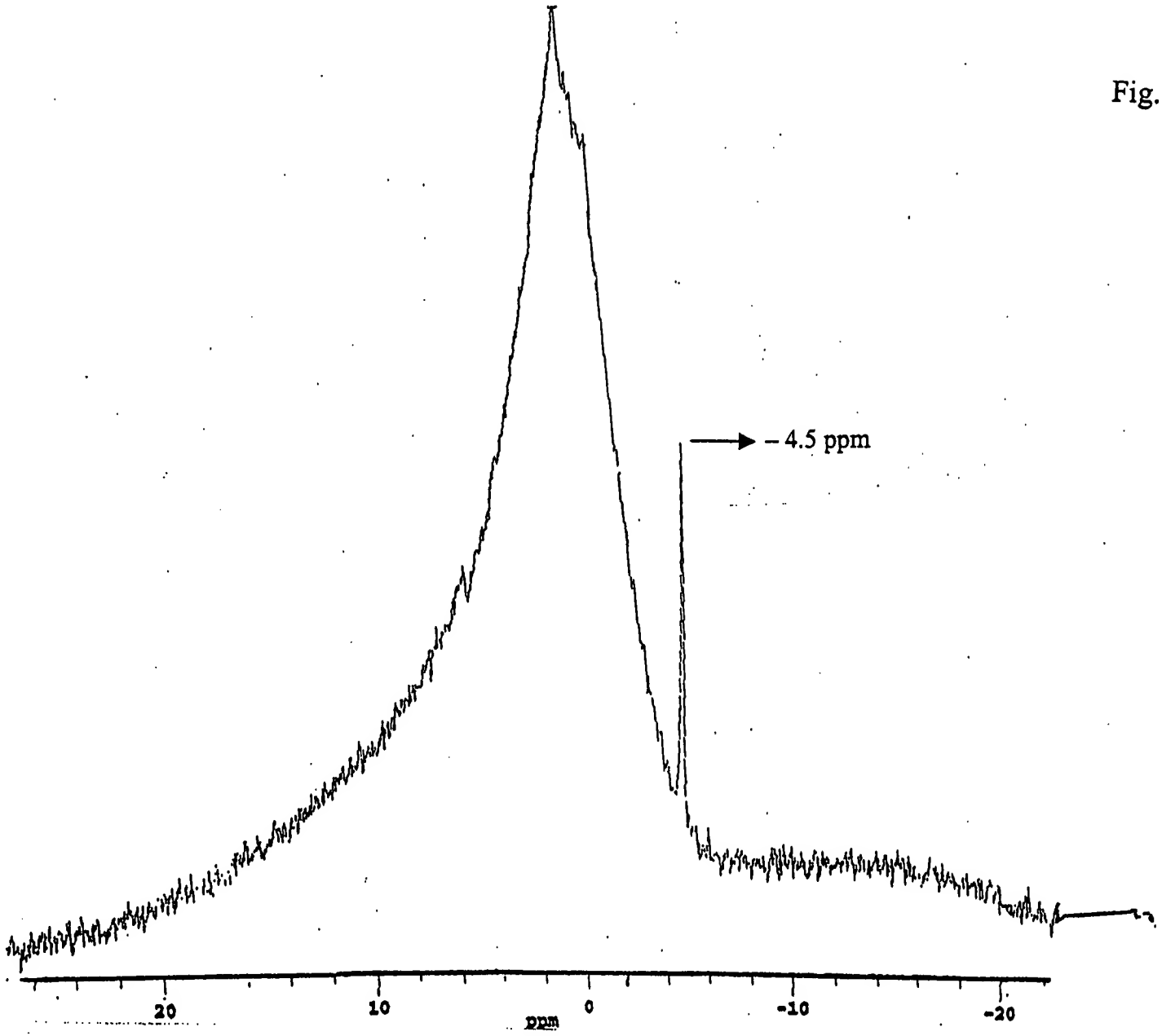

Fig. 13

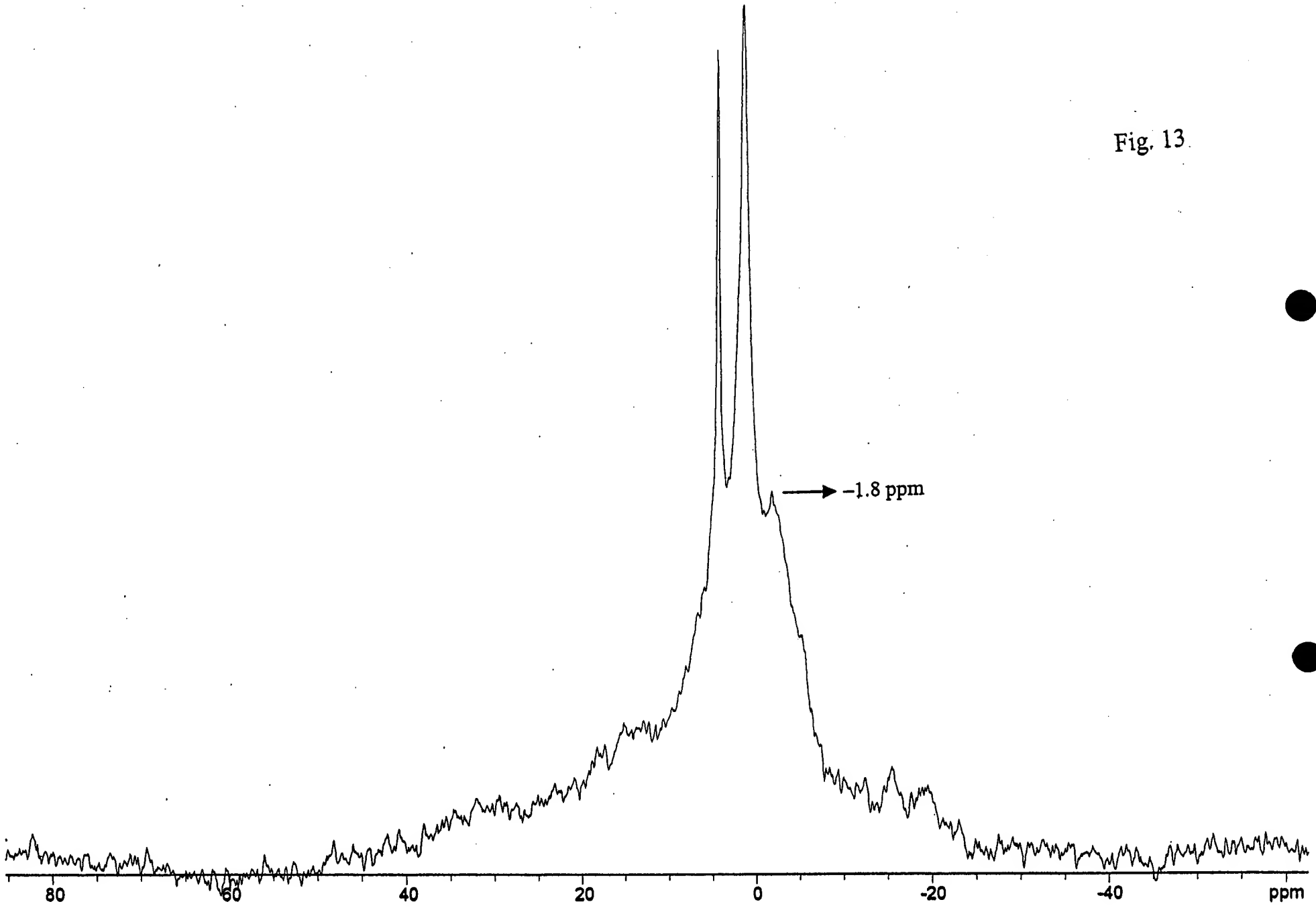

Fig. 14

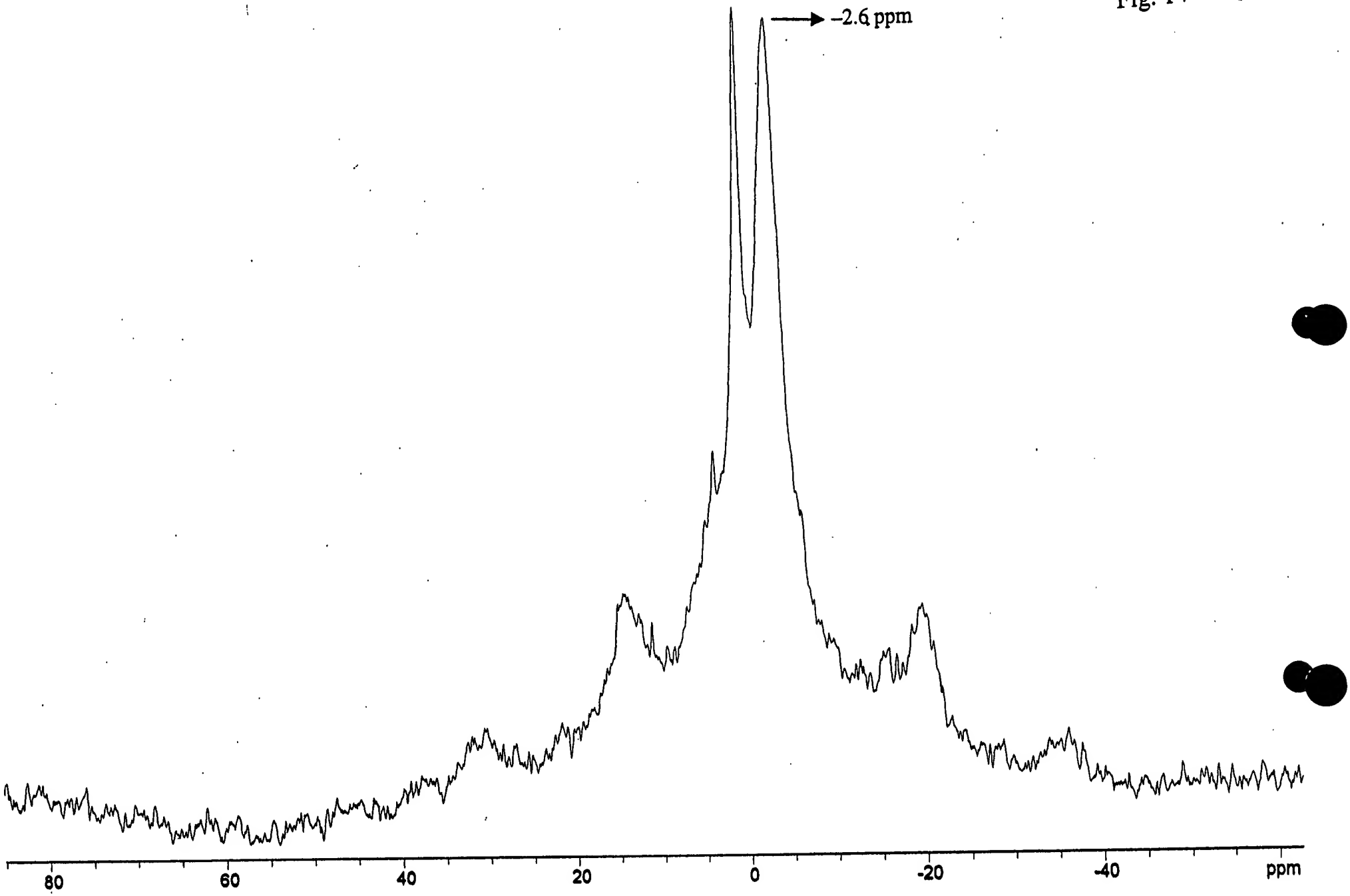

Fig. 15

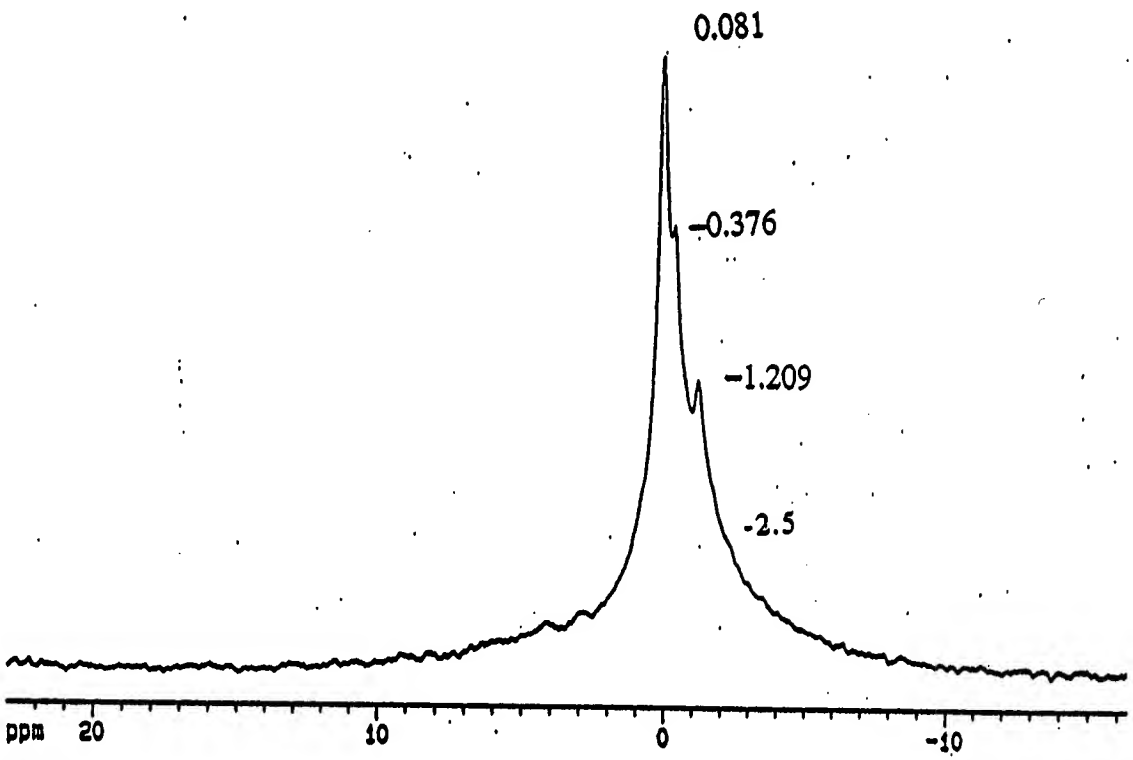

Fig. 16

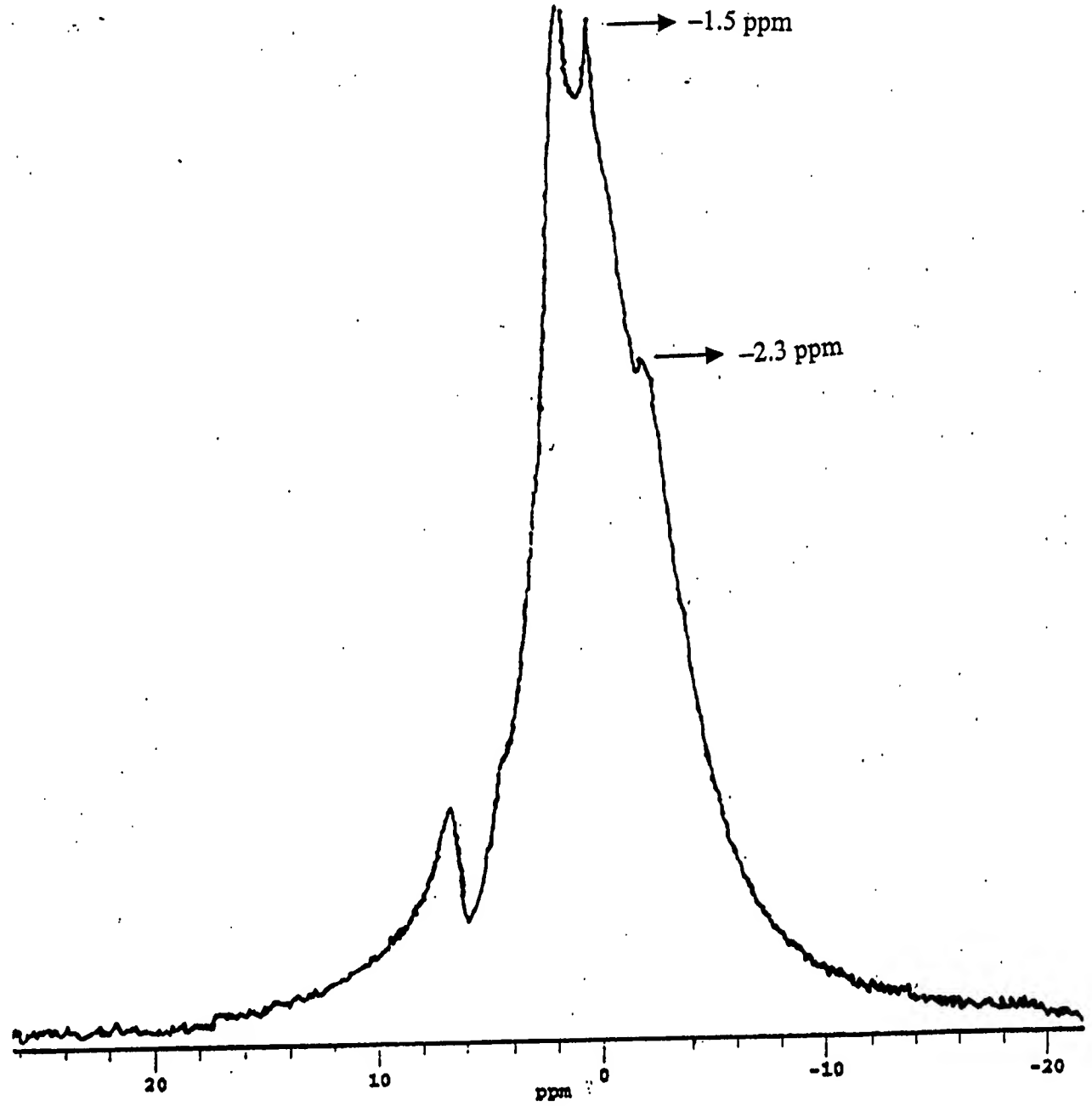

Fig. 17